

---

**Technical Report No: ND08 - 07**

**THE USE OF CHANNEL CHARACTERISTICS  
FOR THE CALIBRATION OF INDEX VELOCITY RATINGS  
FOR ACOUSTIC DOPPLER VELOCITY METERS**

by

**Brent R. Hanson**

**Wei Lin**

**Dept. of Civil Engineering, North Dakota State University  
Fargo, North Dakota**

**November 2008**

**North Dakota Water Resources Research Institute  
North Dakota State University, Fargo, North Dakota**

## Technical Report No: ND08-7

### THE USE OF CHANNEL CHARACTERISTICS FOR THE CALIBRATION OF INDEX VELOCITY RATINGS FOR ACOUSTIC DOPPLER VELOCITY METERS

By

Brent R. Hanson<sup>1</sup>

Wei Lin<sup>2</sup>

WRI Graduate Research Fellow<sup>1</sup> and Associate Professor<sup>2</sup>

Department of Civil Engineering

North Dakota State University

Fargo, ND 58108

November 2008

*This work upon which this report is based was supported in part by federal funds provided by the United State of Department of Interior in the form of ND WRI Graduate Research Fellowship for the graduate student through the North Dakota Water Resources Research Institute.*

*Content of this report do not necessarily reflect the views and policies of the US Department of Interior, nor does mention of trade names or commercial products constitute their endorsement or recommendation for use by the US government.*

Project Period: March 1, 2004 – February 28, 2005

Project Number: 2004ND50B

North Dakota Water Resources Research Institute

Director, G. Padmanabhan

North Dakota State University

Fargo, North Dakota 58105

## TABLE OF CONTENTS

LIST OF FIGURES .....	3
ACKNOWLEDGEMENT .....	6
ABSTRACT .....	6
DESCRIPTION OF WATER PROBLEM ADDRESSED .....	7
BACKGROUND .....	8
Acoustic Doppler Velocity Meter .....	8
Stage-Area Ratings .....	9
Index-Velocity Ratings .....	10
OBJECTIVES .....	11
MATERIALS AND METHODS .....	11
Materials .....	11
Methods .....	12
MODEL DEVELOPMENT .....	13
Dimensional Analysis .....	14
Equations for Index-Velocity Rating .....	14
MODEL CALIBRATIONS AND ASSESSMENTS .....	15
Red River of the North at Grand Forks, ND .....	15
Kankakee River at Davis, IN .....	22
James River at the ND-SD Stateline .....	28
Kootenai River at Tribal Hatchery near Bonners Ferry, ID .....	34
Channel A near Penn, ND .....	41
Big Coulee near Churches Ferry, ND .....	44
CONCLUSIONS .....	49
REFERENCES .....	51

## LIST OF FIGURES

FIGURE 1. ARGONAUT SL, ACOUSTIC DOPPLER VELOCITY METER (ADVM) BY SONTEK.....	8
FIGURE 2. SKETCH OF AN ADVM INSTALLED IN A CHANNEL SETTING (SLOAT AND HULL, 2004). .....	9
FIGURE 3. STAGE-AREA RATING AND MEAN VELOCITY VERSUS INDEX VELOCITY AT IROQUOIS RIVER GAGING STATION NEAR FORESMAN, IND. WITH TRAPEZOIDAL CHANNEL CROSS-SECTION (MORLOCK ET AL. 2002). .....	13
FIGURE 4. STAGE-AREA RATING AND MEAN VELOCITY VERSUS INDEX VELOCITY AT KANKAKEE RIVER AT DAVIS, IND. WITH RECTAGULAR CHANNEL CROSS-SECTION (MORLOCK ET AL. 2002). .....	13
FIGURE 5. MAP OF THE RED RIVER OF THE NORTH (GOOGLE EARTH).....	16
FIGURE 6. PROFILE OF THE RED RIVER OF THE NORTH’S CHANNEL AT GRAND FORKS, ND .....	16
FIGURE 7. DEPTH-AREA RATING FOR THE RED RIVER AT GRAND FORKS, ND .....	17
FIGURE 8. COMPARISON OF MODELED VELOCITY TO MEASURED VELOCITY FOR THE RED RIVER AT GRAND FORKS, ND .....	18
FIGURE 9. COMPARISON OF THE DIFFERENCE BETWEEN THE MODELED VELOCITY AND MEASURED VELOCITY AGAINST THE MEASURED VELOCITY FOR THE RED RIVER AT GRAND FORKS, ND.....	19
FIGURE 10. COMPARISON OF THE SIMPLIFIED MODEL VELOCITY TO THE MEASURED VELOCITY FOR THE RED RIVER AT GRAND FORKS, ND .....	19
FIGURE 11. COMPARISON OF THE TWO VELOCITY MODELS TO THE MEASURED VELOCITY FOR THE RED RIVER AT GRAND FORKS, ND.....	20
FIGURE 12. PLOT OF THE DIFFERENCE BETWEEN THE COMPUTED VELOCITY AND THE MEASURED VELOCITY AGAINST THE MEASURED VELOCITY FOR THE RED RIVER AT GRAND FORKS, ND.....	21
FIGURE 13. COMPARISON OF THE COMPUTED VELOCITIES FROM THE TWO MODELS TO THE MEASURED VELOCITIES COLLECTED SUBSEQUENT TO THE CALIBRATION DATA FOR THE RED RIVER AT GRAND FORKS, ND.....	21
FIGURE 14. PLOT OF THE DIFFERENCE BETWEEN THE COMPUTED VELOCITY AND THE MEASURED VELOCITY AGAINST THE MEASURED VELOCITY COLLECTED AFTER THE CALIBRATION DATA FOR THE RED RIVER AT GRAND FORKS, ND.....	22
FIGURE 15. MAP OF THE KANKAKEE RIVER ADAPTED FROM U.S. GEOLOGICAL SURVEY LANDSAT IMAGERY OBTAINED FROM GOOGLE <sup>TM</sup> EARTH IN 2007.....	22
FIGURE 16. PROFILE OF THE KANKAKEE RIVER’S CHANNEL AT DAVIS, IN. ....	23
FIGURE 17. INDEX-MEAN VELOCITY RELATION FOR THE KANKAKEE RIVER AT DAVIS, IN. ....	23
FIGURE 18. COMPARISON OF MODELED VELOCITY TO MEASURED VELOCITY FOR THE KANKAKEE RIVER AT DAVIS, IN.....	24
FIGURE 19. COMPARISON OF THE DIFFERENCE BETWEEN THE MODELED VELOCITY AND MEASURED VELOCITY AGAINST THE MEASURED VELOCITY FOR THE KANKAKEE RIVER AT DAVIS, IN.....	25
FIGURE 20. COMPARISON OF THE TWO VELOCITY MODELS TO THE MEASURED VELOCITY FOR THE KANKAKEE RIVER AT DAVIS, IN.....	26

FIGURE 21. PLOT OF THE DIFFERENCE BETWEEN THE COMPUTED VELOCITY AND THE MEASURED VELOCITY AGAINST THE MEASURED VELOCITY FOR THE KANKAKEE RIVER AT DAVIS, IN.....	26
FIGURE 22. COMPARISON OF THE COMPUTED VELOCITIES FROM THE TWO MODELS TO THE MEASURED VELOCITIES COLLECTED SUBSEQUENT TO THE CALIBRATION DATA FOR THE KANKAKEE RIVER AT DAVIS, IN. ....	27
FIGURE 23. PLOT OF THE DIFFERENCE BETWEEN THE COMPUTED VELOCITY AND THE MEASURED VELOCITY AGAINST THE MEASURED VELOCITY COLLECTED AFTER THE CALIBRATION DATA FOR THE KANKAKEE RIVER AT DAVIS, IN. ....	27
FIGURE 24. MAP OF THE JAMES RIVER ADAPTED FROM U.S. GEOLOGICAL SURVEY LANDSAT IMAGERY OBTAINED FROM GOOGLE <sup>TM</sup> EARTH IN 2007. ....	28
FIGURE 25. PROFILE OF THE JAMES RIVER’S CHANNEL AT THE ND-SD STATE LINE. ....	28
FIGURE 26. INDEX-MEAN VELOCITY RELATION FOR THE JAMES RIVER AT ND-SD STATE LINE.....	29
FIGURE 27. COMPARISON OF MODELED VELOCITY TO MEASURED VELOCITY FOR THE JAMES RIVER AT ND-SD STATE LINE. ....	30
FIGURE 28. PLOT OF THE DIFFERENCE BETWEEN THE COMPUTED VELOCITY AND THE MEASURED VELOCITY AGAINST THE MEASURED VELOCITY FOR THE JAMES RIVER AT THE ND-SD STATE LINE.....	30
FIGURE 29. INDEX-MEAN VELOCITY RELATION OF THE FIRST 7 MEASURED VELOCITIES FOR THE JAMES RIVER AT THE ND-SD STATE LINE. ....	31
FIGURE 30. COMPARISON OF THE TWO VELOCITY MODELS TO THE MEASURED VELOCITY FOR THE JAMES RIVER AT THE ND-SD STATE LINE. ....	32
FIGURE 31. PLOT OF THE DIFFERENCE BETWEEN THE COMPUTED VELOCITY AND THE MEASURED VELOCITY AGAINST THE MEASURED VELOCITY FOR THE JAMES RIVER AT THE ND-SD STATE LINE.....	32
FIGURE 32. PLOT OF THE DIFFERENCE BETWEEN THE COMPUTED VELOCITY AND THE MEASURED VELOCITY AGAINST THE MEASURED VELOCITY COLLECTED AFTER THE CALIBRATION DATA FOR THE JAMES RIVER AT THE ND-SD STATE LINE.....	33
FIGURE 33. PLOT OF THE DIFFERENCE BETWEEN THE COMPUTED VELOCITY AND THE MEASURED VELOCITY AGAINST THE MEASURED VELOCITY COLLECTED AFTER THE CALIBRATION DATA FOR THE JAMES RIVER AT THE ND-SD STATE LINE.....	33
FIGURE 34. MAP OF THE KOOTENAI RIVER ADAPTED FROM U.S. GEOLOGICAL SURVEY LANDSAT IMAGERY OBTAINED FROM GOOGLE <sup>TM</sup> EARTH IN 2007. ....	34
FIGURE 35. PROFILE OF THE KOOTENAI RIVER AT THE TRIBAL HATCHERY NEAR BONNERS FERRY, ID. ....	34
FIGURE 36. DEPTH-AREA RATING FOR THE KOOTENAI RIVER AT THE TRIBAL HATCHERY NEAR BONNERS FERRY, ID.....	35
FIGURE 37. COMPARISON OF THE CROSS-SECTIONAL MODEL TO THE LAYOUT OF THE CROSS-SECTION. ....	36
FIGURE 38. INDEX-MEAN VELOCITY RELATION FOR THE KOOTENAI RIVER AT TRIBAL HATCHERY NEAR BONNERS FERRY, ID.....	36
FIGURE 39. COMPARISON OF MODELED VELOCITY TO MEASURED VELOCITY FOR THE KOOTENAI RIVER AT TRIBAL HATCHERY NEAR BONNERS FERRY, ID.....	37

FIGURE 40. PLOT OF THE DIFFERENCE BETWEEN THE COMPUTED VELOCITY AND THE MEASURED VELOCITY AGAINST THE MEASURED VELOCITY FOR THE KOOTENAI RIVER AT TRIBAL HATCHERY NEAR BONNERS FERRY, ID. ....37

FIGURE.41. INDEX-MEAN VELOCITY RELATION OF THE FIRST 10 MEASURED VELOCITIES FOR THE KOOTENAI RIVER AT TRIBAL HATCHERY NEAR BONNERS FERRY, ID. ....38

FIGURE.42. COMPARISON OF THE TWO VELOCITY MODELS TO THE MEASURED VELOCITY FOR THE KOOTENAI RIVER AT TRIBAL HATCHERY NEAR BONNERS FERRY, ID. ....39

FIGURE 43. PLOT OF THE DIFFERENCE BETWEEN THE COMPUTED VELOCITY AND THE MEASURED VELOCITY AGAINST THE MEASURED VELOCITY FOR THE KOOTENAI RIVER AT TRIBAL HATCHERY NEAR BONNERS FERRY, ID. ....39

FIGURE 44. ONE TO ONE COMPARISON OF THE COMPUTED VELOCITIES TO THE MEASURED VELOCITIES FOR THE KOOTENAI RIVER AT TRIBAL HATCHERY NEAR BONNERS FERRY, ID. ....40

FIGURE 45. PLOT OF THE DIFFERENCE BETWEEN THE COMPUTED VELOCITY AND THE MEASURED VELOCITY AGAINST THE MEASURED VELOCITY COLLECTED AFTER THE CALIBRATION DATA FOR THE KOOTENAI RIVER AT TRIBAL HATCHERY NEAR BONNERS FERRY, ID. ....40

FIGURE 46. MAP OF CHANNEL A NEAR PENN, ND AND BIG COULEE NEAR CHURCHES FERRY, ND ADAPTED FROM U.S. GEOLOGICAL SURVEY LANDSAT IMAGERY OBTAINED FROM GOOGLE™ EARTH IN 2007. ....41

FIGURE 47. INDEX-MEAN VELOCITY RELATION FOR CHANNEL A NEAR PENN, ND. ....42

FIGURE 48. COMPARISON OF THE MODELED VELOCITY TO MEASURED VELOCITY FOR CHANNEL A NEAR PENN, ND. ....43

FIGURE 49. COMPARISON OF THE TWO VELOCITY MODELS TO THE MEASURED VELOCITY FOR.....44

FIGURE 50. PLOT OF THE DIFFERENCE BETWEEN THE COMPUTED VELOCITY AND THE MEASURED VELOCITY AGAINST THE MEASURED VELOCITY FOR CHANNEL A NEAR PENN, ND. ....44

FIGURE 51. PROFILE OF THE CHANNEL CROSS-SECTION FOR BIG COULEE NEAR CHURCHES FERRY, ND.....45

FIGURE 52. DEPTH-AREA RATING FOR BIG COULEE NEAR CHURCHES FERRY, ND.....45

FIGURE 53. COMPARISON OF THE CROSS-SECTIONAL MODEL TO THE LAYOUT OF THE CROSS-SECTION FOR BIG COULEE NEAR CHURCHES FERRY, ND. ....46

FIGURE 54. INDEX-MEAN VELOCITY RELATION FOR THE BIG COULEE NEAR CHURCHES FERRY, ND.....46

FIGURE 55. COMPARISON OF MODELED VELOCITY TO MEASURED VELOCITY FOR BIG COULEE NEAR CHURCHES FERRY, ND.....47

FIGURE 56. COMPARISON OF THE TWO VELOCITY MODELS TO THE MEASURED VELOCITY FOR BIG COULEE NEAR CHURCHES FERRY, ND. ....48

FIGURE 57. PLOT OF THE DIFFERENCE BETWEEN THE COMPUTED VELOCITY AND THE MEASURED VELOCITY AGAINST THE MEASURED VELOCITY FOR BIG COULEE NEAR CHURCHES FERRY, ND.....48

## **ACKNOWLEDGEMENT**

Stipend support for the Research Fellow, Brent R. Hanson, was provided by the North Dakota Water Resources Research Institute. We thank the US Geological Survey North Dakota Water Science Center for providing the equipment, and Skip Vecchia, Bill Damschen and Jason Lambrecht for their expertise and assistance throughout this study. Appreciations are conveyed to Dr. G.Padmanaban, Gregg Wiche and Dr. Peter Oduor for their technical advises.

## **ABSTRACT**

Acoustic Doppler Velocity Meters (ADVMS) have become popular for estimating discharge in rivers exhibiting complex flow characteristics. To use the ADVMS for estimating channel discharge, a relation needs to be developed between the mean channel velocity and the index velocity provided by the ADVMS. In the past, this relation was primarily developed empirically. To improve the accuracy of ADVMS discharge estimates, a more theoretical approach was developed for defining the relationship between a river's mean channel velocity and the ADVMS's index velocity. This approach involves using the channel's geometry at a single cross-section to more accurately define the mean channel velocity to index velocity relation by means of fewer discharge measurements. The use of the channel geometry allows for a more theoretical explanation of the mean-index velocity relation, whether linear or nonlinear, resulting in a more accurate extrapolation of the rating.

## DESCRIPTION OF WATER PROBLEM ADDRESSED

As the Nation's population continues to grow and the countryside continues to become more and more developed, the importance of having accurate real-time river discharge data becomes more and more significant for government agencies and private companies. Real-time discharge data are required so that the best water management practices can be swiftly put in place for flood control, water distribution, and drought management tactics (Mason and Weiger, 1995). The United States Geological Survey (USGS) provides a large percentage of the needed data. The USGS is a government agency that operates more than 7,000 stream-gaging stations across the nation, which provides more than 85% of the country's discharge information (Mason and Weiger, 1995, and Hirsch and Norris, 2001). Of the 7,000 plus stations, well over 4,000 of those are monitored in real-time (Wahl *et al*, 1995). The USGS strives to provide the most accurate data possible and continually implements technologies that aide in carrying out this objective.

Throughout the years, numerous methods have been developed to estimate discharge. Historically, the most commonly used method is the "stage-discharge" relation (Morlock *et al*, 2002). This method, known as the "conventional method", estimates discharge based on the rise and fall of the channel's water level. The conventional method provides satisfactory results for many stream-gaging stations (Rantz and others, 1982). For stations with complex flow conditions, estimating discharge using the conventional method becomes impractical (Morlock *et al*, 2002). For these situations, different method needs to be used to estimate discharge.

In recent years, there has been an increasing interest in the use of hydroacoustic principles to monitor water flow. There have been many different models developed for different situations. One system that uses these principles is the Acoustic Doppler Velocity Meter (ADVM). An ADVM is a small, non-intrusive piece of equipment that can easily be installed into a river or stream setting (Sloat and Hull, 2004). The ADVM provides a sample velocity (also known as the "index" velocity) within a portion of a river. The index velocity can then be related to the mean channel velocity and used in discharge computation. The implementation of this equipment can make it practical to produce discharge records at sites where previously used methods were unrealistic (Morlock *et al*, 2002).

As of Feb 2001, over 150 ADVM units had been purchased by the USGS to aide in stream-gaging (Morlock *et al*, 2002). From 2001 to the present date, that total has increased greatly as ADVMs have become more and more popular. The velocity calibration process for the ADVM is mainly empirical, requiring numerous discharge measurements until ADVM's velocities become useful. This is due to the empirical methods requiring a range of mean channel and index velocities to be measured in order to develop a relation between the two. This relation can take time to develop and consequently impedes the use of the ADVM for discharge computation. Therefore the development of a more theoretical method of calibration can deliver a more rapid index-mean velocity relation, expediting the ADVM's implementation into computation of discharge and in turn, improving discharge estimation during complex flow conditions.

In this research an analytical relationship between the channel's mean velocity and ADVM's index velocity was developed. The model includes the channel cross-section geometry and has a



potential to be used for channels with wide ranges of cross-sectional shapes. The model was successfully applied to calibrate ADVm data collected from 6 gaging sites.

## BACKGROUND

### Acoustic Doppler Velocity Meter (ADVm)

An ADVm is a small, non-intrusive piece of equipment that can easily be installed into a river or stream setting. ADVms, as pictured in Figure 1, have been found to provide reliable index velocities that can be used to produce a more accurate discharge estimate when properly calibrated (Morlock, et al, 2002). An ADVm uses a pair of monostatic acoustic transducers set at a known angle in a plane that is parallel to the water surface to measure water velocities. Each transducer transmits sound pulses of a known frequency along a narrow “acoustic beam”. When sound pulses strike particulate matter suspended in the water, some of the sound is reflected back to the transducer. Flow velocity is determined based on the frequency (Doppler) shift which is proportional to the velocity of the water in which particulate matter is traveling along. From velocities measured by the two transducers, ADVm computes a mean velocity (index velocity) in a sample volume defined by the user. The velocity is output in terms of an x-component (along the flow direction) and y-component (perpendicular to the flow).



Figure 1. Argonaut SL, Acoustic Doppler Velocity Meter (ADVm) by SonTek

Typically, the ADVm is mounted in a horizontal position, from which it is able to continually monitor the velocities at a set stage across the channel’s velocity profile. It has to be installed at a height below the minimum water level and facing perpendicular to the stream flow direction. The average velocity within the sample volume of the main channel is recorded as an index velocity. As shown in Figure 2, the ADVm may provide a non-intrusive method of measuring a channel’s flow velocity with fewer limitations than previously used methods (Sloat and Hull, 2004). This allows for more accurate discharge estimates for a wider range of hydraulic conditions without disturbing the natural flow patterns within the channel.

The fundamental assumption of the index-velocity rating method is that there exists a well-defined relation between the velocity found within the sample volume and the mean-velocity in the cross-section (Sloat and Hull (SonTek), 2004). With the index-velocity rating and cross-section area known for various stages, discharge (Q) may be calculated using the velocity (V)-area (A) method

$$Q = \bar{V}A \quad (1)$$

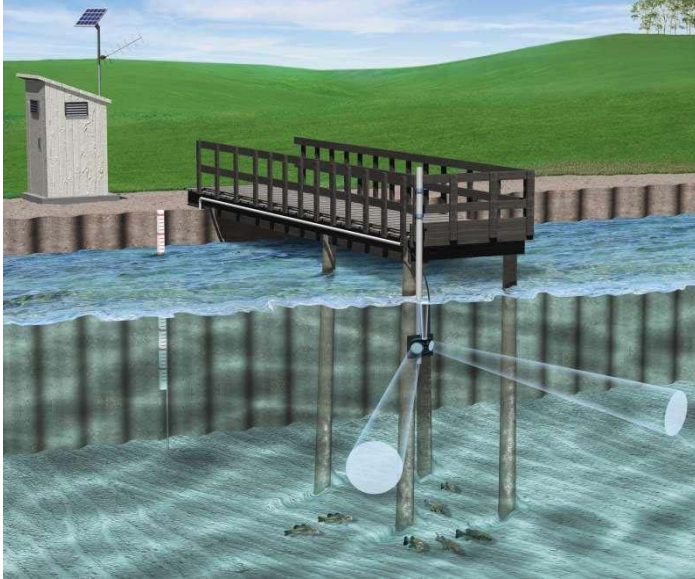


Figure 2. Sketch of an ADVM installed in a channel setting (Sloat and Hull, 2004).

### Stage-Area Ratings

Stage-area rating refers to the channel cross-section area ( $A$ ) change as a function of river stage ( $s$ ) at a gaging station. The stage-area rating is determined from detailed channel survey. Variety techniques have been used for channel surveys. These techniques include sounding weights, fathometers, downward-looking acoustic Doppler current profilers (ADCPs), and standard land surveying techniques to characterize the river cross-section profile (Ruhl and Simpson, 2005). There are a number of approaches that have been used to develop stage-area ratings, such as, empirical curve fittings, geometric equations, and computer programs such as AREACOMP. One of the conventional methods for stage-area rating is through development of standard cross-sections (Morlock, 2002). A standard cross-section can be developed by approximating the channel profile with a combination of sections of straight lines. The purpose of this step is to produce a simpler geometric shape to facilitate the computation of the channel's cross-sectional area in relation to a given stage.

Rectangular and trapezoidal are most commonly used shapes for the development of stage-area ratings. When the bottom elevation is known, water depth ( $y$ ) in the channel can be easily calculated from stage. Using channel bottom as the datum, stage-area rating for rectangular and trapezoidal cross-sections can be presented as,

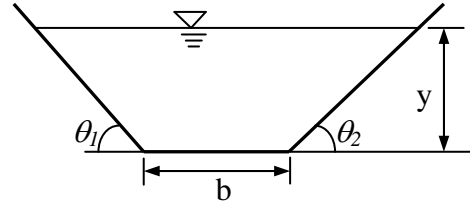
*Rectangular cross-section area ( $A$ ),*

$$A = by$$

Where  $b$  is channel bottom width and  $y$  is water depth.

Trapezoidal cross-section area ( $A$ ),

$$A = \frac{1}{2 \tan \theta_1} y^2 + \frac{1}{2 \tan \theta_2} y^2 + by$$



Since  $\theta_1$  and  $\theta_2$  are constant for a given channel cross-section, above equation can be written as,

$$A = my^2 + by \quad (2)$$

Where

$$m = \frac{1}{2 \tan \theta_1} + \frac{1}{2 \tan \theta_2}$$

For the purpose of simplification, the bank slopes for the channels used for this study are assumed to be equal for both sides.

### Index-Velocity Ratings

An index velocity rating represents the relation between the index velocity measured by an ADVm and the mean channel velocity. After a rating curve is established, mean velocities can be computed from the ADVm velocities recorded at a station. Successful establishment of this relationship is the basis for more accurate discharge estimates using the velocity-area method (Equation. 1).

To develop index velocity ratings, concurrent ADVm velocities and mean channel velocities need to be collected. The mean velocity of the river can be derived by first dividing a cross-section of a stream into sub-sections and measuring the average velocity in each sub-section. Sub-sectional discharges can then be calculated by multiplying the average velocity of the sub-section by the area of the sub-section. The total discharge for the channel is found by the sum of the sub-sectional discharges and the total area of the cross-section is found by summing the sub-areas. A weighted mean velocity for the channel is then computed by dividing the total discharge by the total area. The technique of dividing up the cross-section used by the USGS is known as the midsection method (Rantz and others, 1982). Instruments that are used for velocity measurement include rotating-cup current meters and ADCP's.

Multiple measurements for a range of discharges and stages are required to develop an index velocity rating. Common practice in developing index velocity rating is plot the mean velocity versus index velocity from a series of measurements on an x-y plot. The index-velocity rating is developed by finding a best fit line or curve, mathematic expressions, to scatter plot points. Selection of the mathematic equations is only dependent on the shape of the plot. In many cases, linear fits (Equation. 3) provide satisfactory results, and for others, the relation may be best described as curvilinear or as a compound curve (Equation. 4) (Morlock, et al., 2002).

Linear relation: 
$$\bar{V} = XV_i + C \quad (3)$$

Curvilinear relation: 
$$\bar{V} = V_i(X + YH) + C \quad (4)$$

where,  $\bar{V}$  is the computed mean velocity,

$\bar{V}_i$  is the index velocity measured by ADVM

$X$  is the velocity coefficient

$Y$  is the stage coefficient

$H$  is the stage, and

$C$  is a constant

No discussion on how flow conditions and channel cross-section geometry may affect the mean velocity and index velocity is found in literature.

## OBJECTIVES

The goal of this study was to improve and hasten the use of ADVMs that have been implemented into stream-gaging situations. Specific objectives of this research included:

- Analyzing various the methods of estimating and computing discharge,
- Reviewing previous studies conducted on the use of ADVMs for computing discharge estimates and the studies short comings,
- Reviewing previous studies conducted on the role channel geometry has on velocity relations within the channel,
- Acquisition and collection of field data for several rivers. Included with the field data is discharge, mean channel velocity, ADVM index velocity and profile of the channel cross-section,
- Development of an index-mean velocity model that allows for the development of an accurate velocity rating with fewer discharge measurements, and
- Evaluation of the effectiveness of the newly derived model in comparison with the methods currently in use.

## MATERIALS AND METHODS

### Materials

#### ADVMs

Every USGS gaging station used for this study was equipped with a 1.5 and 0.5 MHz ADVM produced by Sontek® Inc. The 1.5 MHz model is able to measure within the range of 0.7 to 66 ft and the 0.5 MHz model can be set to measure within the range of 5 to 400 ft. Depending on the size of channel, a model can be selected to serve the desired purpose.

The Argonaut –SL can measure velocities ranging from 0.00-20 ft/s (Sontek Corporation, 2004). Within this range, the ADVMs accuracy is within +/- 1% of the measured velocity, +/- 0.015 ft/s. The ADVM also has a resolution of 0.003 ft/s. The design of these ADVMs allows for the instruments to provide a reliable index velocity for a range of hydraulic conditions.

### **Discharge Measurements**

Discharge measurements were conducted at each site for the calibration of the index-mean velocity rating. Discharge measurements were made using one of two methods.

One uses a Price AA current meter to collect point velocities and uses the midsection method as described by Rantz and Others (1982) to compute discharge. This method commonly referred to as the conventional current-meter method.

The other method used to obtain discharge is by means of an Acoustic Doppler Current Profiler (ADCP). ADCPs use acoustic signals to simultaneously measure velocity and depth across the channel and use this data to compute discharge.

Discharges from both methods are considered valid and the method used for each measurement is based on channel conditions and the equipment available for use.

### **Channel Cross-section Data**

Channel cross-section data for four of the sites was obtained using a surveyor's level to establish stage elevation points on the bridge the ADVN is mounted. A sounding weight is then used to determine the elevation of the channel bed below each elevation point.

For the remaining two sites, channel bed elevations were determined using an ADCP and the water depth data collected during a discharge measurement.

### **Stage-Area Ratings**

Stage-area ratings were developed using the computer program AREACOMP (Ruhl and Simpson, 2005) and channel bed elevation data collected for the channel cross-section.

### **Velocity Ratings**

Index-mean velocity ratings were calibrated using the spreadsheet EXCEL by Microsoft®.

### **Methods**

For the collection of index velocities and mean channel velocities, the ADVN was programmed to continually record velocities within the ADVN's set sample volume. Simultaneous to the ADVN's data collection, the discharge within the river is measured by means of the conventional current-meter method or by means of an ADCP. After the discharge in the channel is measured, the mean channel velocity is determined by dividing the measured discharge by the area obtained from the stage-area rating for the ADVN cross-section. The mean channel velocity is linked to the index velocity recorded by the ADVN. This process is repeated for a range of flows to collect sufficient velocity data for the calibration of the models.

For this project, a portion of the data collected for four of the six sites was collected personally in conjunction employees of the ND Water Science Center. Data for the sites located in Idaho and Indiana was provided by the respective state's Water Science Center.

After the discharge data and ADVM data is collected, the data is entered into an EXCEL spreadsheet. This data includes depth of discharge measurement, mean channel velocity, and the index velocity provided by the ADVM. Using the spreadsheet, the constants for the model are then calibrated by minimizing the sum of the squared differences between the measured mean channel velocity and the computed mean channel velocity.

## MODEL DEVELOPMENT

One of the early reports on using ADVM and the index velocity rating for river discharges were made by Morlock et al. (2002) based on their studies of three rivers in Indiana. Comparison of the index-velocity ratings with stage-area ratings of the rivers studied by Morlock et al. showed interesting relations. For trapezoidal channels, cross-section area increases follows a quadratic relation with the increase of stage, while linear relation between the mean channel velocity and index velocity is observed (Figure 3). For rectangular channels, cross-section area increases linearly with the stage, but a non-linear (curvilinear) relation holds (Figure 4).

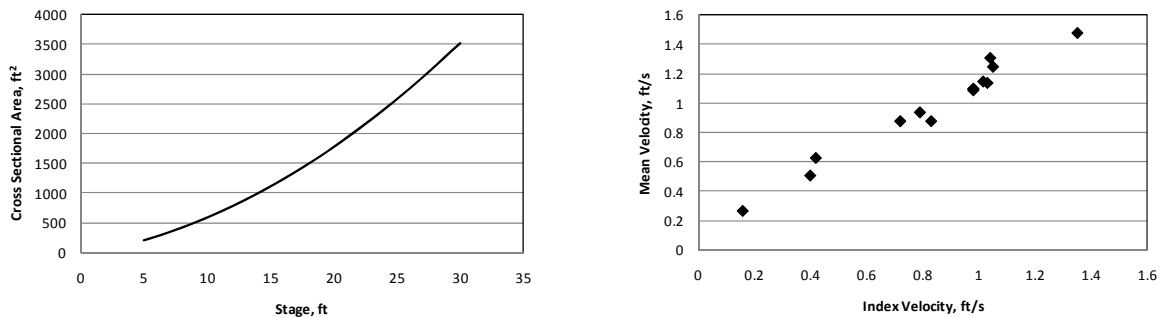


Figure 3. Stage-area rating and mean velocity versus index velocity at Iroquois River gaging station near Foresman, Ind. with trapezoidal channel cross-section (Morlock et al. 2002).

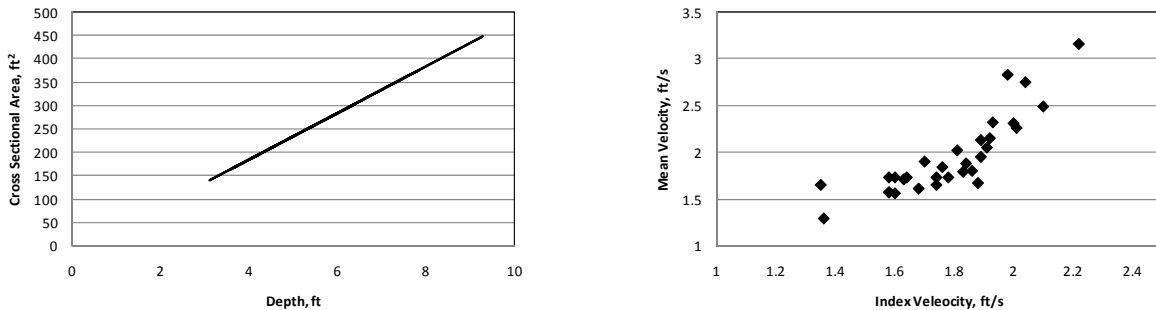


Figure 4. Stage-area rating and mean velocity versus index velocity at Kankakee River at Davis, Ind. with rectangular channel cross-section (Morlock et al. 2002).

Further analysis of Figures 3 and 4 showed that when the stage-area rating is combined with the index-velocity rating, discharge (cross-section times mean velocity) is a function of water depth and index velocity. It is hypothesized that discharge can be expressed as a function of index velocity and river stage (H) or depth (y) and this expression will be applicable to all channel cross-section profiles.

$$Q = f(V_i, y) \quad (5)$$

### Dimensional Analysis

To define the mathematical relation for discharge as a function of index velocity and water depth, dimensional analysis was applied. Equation 5 may be written as

$$Q = KV_i^a y^b \quad (6)$$

Substituting the dimensional formulae for the variables involved, K is eliminated and following relationship is derived

$$L^3T^{-1} = (LT^{-1})^a L^b \quad (7)$$

By equating first the exponents of the fundamental quantity length and then the exponents of the fundamental quantity time, dimensional homogeneity of the equation is achieved (Huntley, 1955). Thus:

$$\text{(length)} \quad 3 = a + b$$

$$\text{(time)} \quad -1 = -a$$

$$\text{therefore} \quad a = 1, b = 2$$

$$\text{and hence} \quad Q = KV_i y^2 \quad (8)$$

### Equations for Index-Velocity Rating

$$\text{Since} \quad Q = A\bar{V}$$

$$\text{where} \quad A = \text{channel cross-section area}$$

$$\bar{V} = \text{mean channel flow velocity}$$

Equation 8 can be rearranged to establish a  $\bar{V}$  and  $V_i$  relation, the rating curve. Thus,

$$\bar{V} = K \frac{V_i y^2}{A} \quad (9)$$

Cross-section area ( $A$ ) is a function of channel geometry and water depth ( $y$ ). For most commonly used channel cross-section geometries, rectangular and trapezoidal, Equation 9 may be written as follows,

*Index-Velocity Rating for Rectangular Channel Cross-sections*

Since  $A = by$

Then 
$$\bar{V} = K \frac{V_i y^2}{by} = K \frac{V_i y}{b} \quad (10)$$

Equation 10 shows that for rectangular channels, the mean velocities linear relationship to the index velocity, is proportional to water depth and is inversely proportional to the channel bottom width. Since channel bottom width is a constant, mean velocity tends to change in a nonlinear pattern as water depth and index velocity change. This result is in agreement with the curvilinear model proposed by Morlock et al (2002). Please note that in Equation 10 water depth instead of stage level was used.

*Index-Velocity Rating for Trapezoidal Channel Cross-sections*

Since  $A = (my + b)y$

Then 
$$\bar{V} = K \frac{V_i y^2}{(my + b)y} = K \frac{V_i y}{my + b} \quad (11)$$

Similar to the equation for rectangular channels, mean velocity is a function of both index velocity and water depth. Because channel width changes with water depth, channel slopes also have to be included. Equation 11 may be simplified when water is deep enough so that  $my$  is significantly greater than  $b$ . Under such situations, Equation 11 may be simplified as

$$\bar{V} \approx K \frac{V_i}{m} = K' V_i \quad (12)$$

where,  $K' = \frac{K}{m}$

Equation 12 shows a linear relation between mean velocity and index velocity. This may explain why linear index-velocity ratings have been successfully used for most trapezoidal channel flows.

**MODEL CALIBRATION AND ASSESSMENT**

**Red River of the North at Grand Forks, ND**

The Red River of the North (hereafter Red River) is a river that starts at the confluence of the Bois de Sioux and Otter Tail Rivers in Southern North Dakota and Minnesota. From there it meanders north and empties into Lake Winnipeg in Canada as seen in Figure 5.



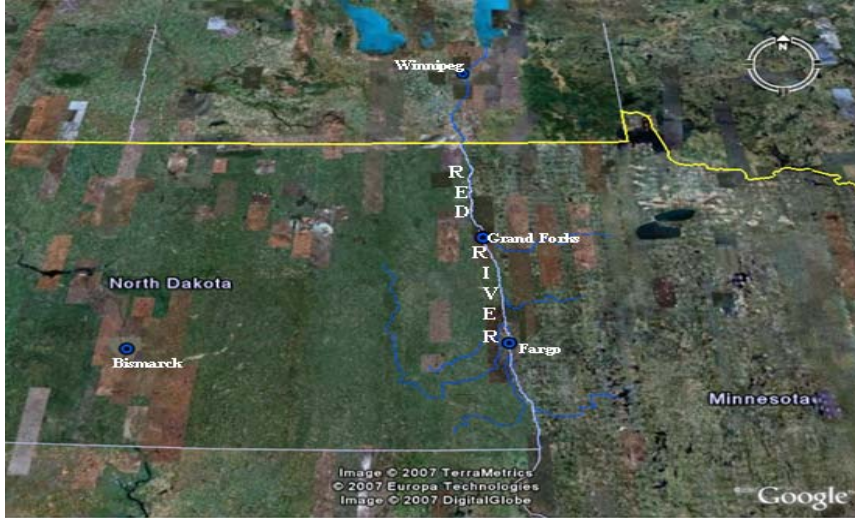


Figure 5. Map of the Red River of the North (Google Earth)

The average slope of the river’s channel is only 0.0002 ft/ft between Fargo and Grand Forks, North Dakota and decreases in slope downstream. This then results in periods of variable backwater and other complex flow conditions. These flow conditions made discharge difficult to compute based on stage alone. To aide in more accurately estimating discharge, the USGS gaging station, Red River at Grand Forks, was selected to be equipped with an ADVN. The ADVN was installed in March 2001.

**Channel Geometry of the Red River at Grand Forks, ND**

The Red River has a meandering channel with a firm bed and sloping banks that lead up to the flood plain. The cross-sectional geometry of the river at Grand Forks can be generalized as trapezoidal or triangular as seen in Figure 6.

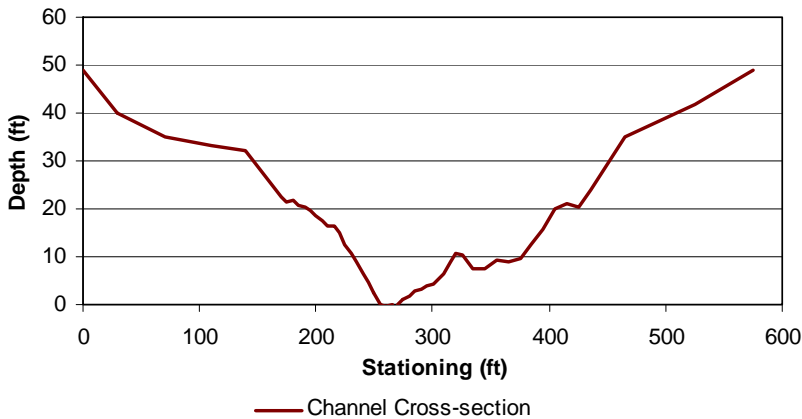


Figure 6. Profile of the Red River of the North’s Channel at Grand Forks, ND

The trapezoidal form of geometry can explain the nonlinear relation in the depth-area rating. The depth-area rating is developed by means of surveying the channel cross-section. The cross-sectional survey is then used to compute the area corresponding to a given depth. The nonlinear relation that develops for the Red River at Grand Forks can be seen in Figure 7.

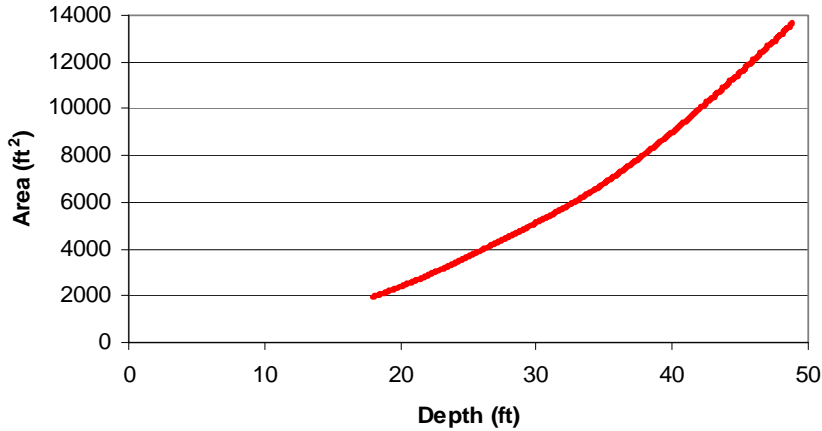


Figure 7. Depth-Area Rating for the Red River at Grand Forks, ND  
 The depths along with the corresponding areas were used to fit the data to the linear model given by Equation 13 for trapezoidal cross-section.

Rearrange Equation 2,  $A = my^2 + by$ , yields a linear equation (Equation 13)

$$\frac{A}{y} = my + b \quad (13)$$

Linear regression between the depth ( $y$ ) of flow and the corresponding area:depth ratio ( $A/y$ ) fits the data with the following result.

$$\frac{A}{y} = 5.4127y + 9.9421 \quad (14)$$

The linear fit has a strong correlation with an  $R^2$  value of 0.997. From the above equation, the channel bottom width was determined to be 9.9 ft. With an  $m$  value of 5.4127, the average slopes for both sides equate to be around  $10.5^\circ$ . Fitted channel cross-section and field data are shown in Figure 8.

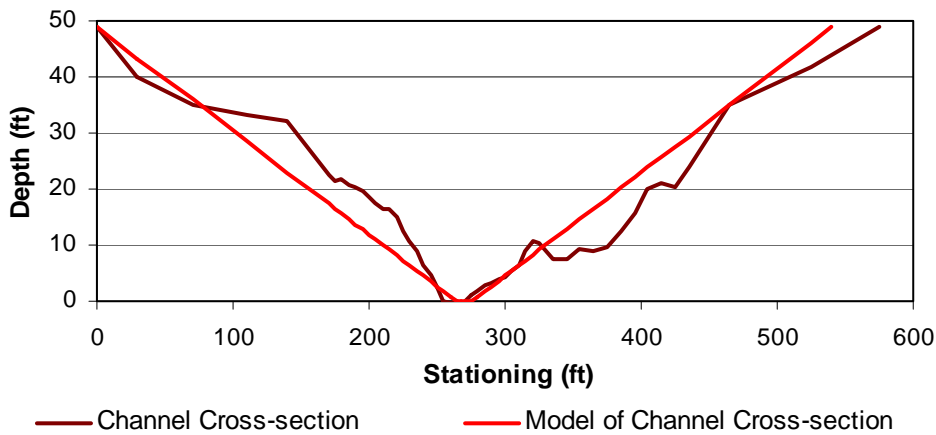


Figure 8. Comparison of the cross-sectional model to the layout of the cross-section.

### Channel Geometry Based Velocity Rating for the Red River at Grand Forks, ND

The trapezoidal velocity rating model, Equation. 11, was applied to develop an index-mean velocity rating for the channel. Using the velocity and stage data from the field, the model was calibrated. Calibration of the model was started by substituting fitted cross-section geometrical parameters into Equation. 11.

$$V_{Mean} = K \frac{y(V_{Index})}{5.4127y + 9.9421} \quad (15)$$

The  $K$  value for the model was derived by minimizing the sum of the squared differences between the measured velocities and the computed velocities. The  $K$  value derived through the regression process was found to be 4.83.

$$V_{Mean} = 4.83 \frac{y(V_{Index})}{5.4127y + 9.9421} \quad (16)$$

Mean channel velocities calculated using the above relationship are presented in Figure 7 together with the field data. The index-mean velocity rating provides a good fit to the measured velocity data. The coefficient of determination for the Equation 16 was found to be:  $R^2 = 0.981$ .

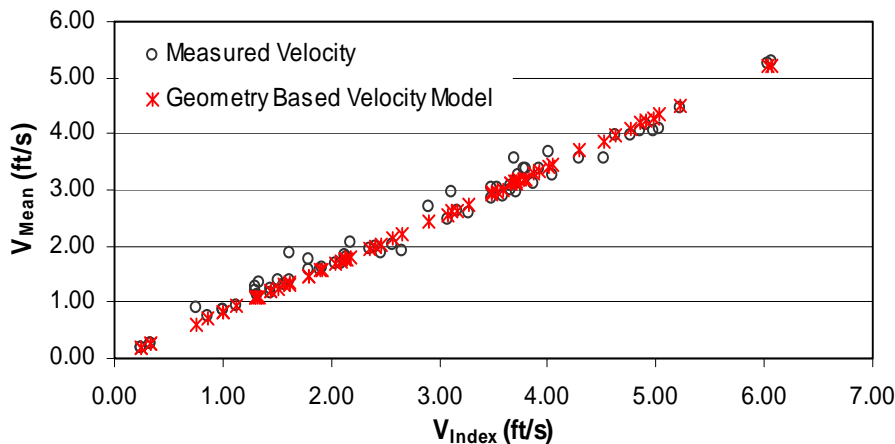


Figure 8. Comparison of modeled velocity to measured velocity for the Red River at Grand Forks, ND

The differences between model results and measured mean velocities are plotted versus measured channel mean velocity, as shown in Figure 8. There appears to be no clear trend of deviation from the measured velocity. The model provided unbiased estimates within the range of calibration as seen with Figure 9.

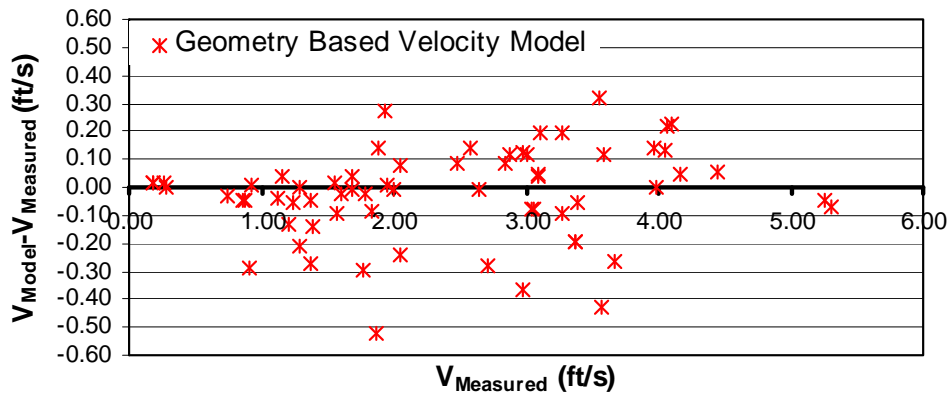


Figure 9. Comparison of the difference between the modeled velocity and measured velocity against the measured velocity for the Red River at Grand Forks, ND

**Simplification of the Calibrated Channel Geometry Based Velocity Rating**

As discussed earlier, when channel bottom width ( $b$ ) is significantly smaller than water depth, the rating curve for trapezoidal cross-section may be simplified as a linear model (Equation. 12). Channel cross-section of the Red River at Grand Forks, ND has a channel bed width estimated to be around 10 ft. For the range of flows within the channel, the depth varied from 20 to 50 ft. Based on this,  $my \gg b$  becomes true. Therefore the index-velocity rating can be simplified to the linear form. Calibrated simplified model is shown as Equation. 17, with a coefficient of determination of  $R^2 = 0.971$ , which slightly lower than that of the model without simplification. Model simulation results and field data are plotted in Fig. 10 for comparison.

$$V_{Mean} = 0.89(V_{Index}) \tag{17}$$

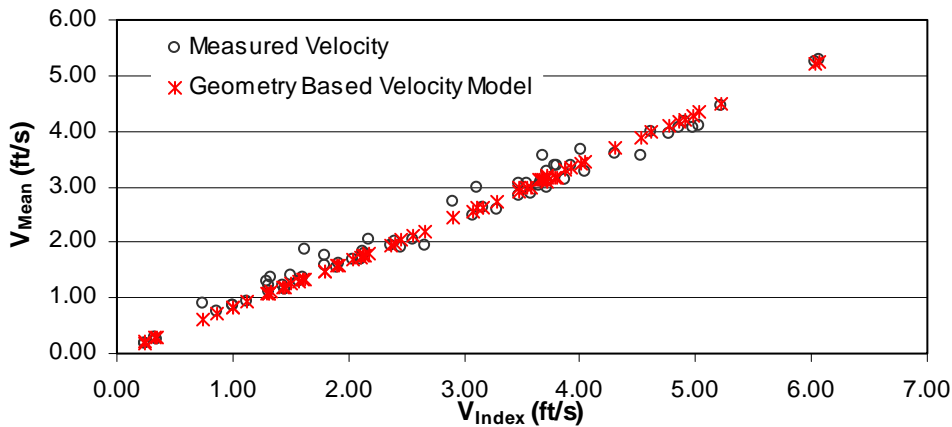


Figure 10. Comparison of the simplified model velocity to the measured velocity for the Red River at Grand Forks, ND

**Comparison of the Channel Geometry-Based Velocity Rating and the Established Rating for the Red River at Grand Forks, ND**

For the Red River at Grand Forks, ND, linear regression has been the method used for modeling the relation. The channel geometry-based velocity rating is compared to the velocity rating developed through linear regression. For this comparison, both velocity ratings are calibrated using the same data sets.

To develop the first velocity rating for the Red River at Grand Forks, the first 20 velocity measurements were used. These measurements were conducted within a time period from April 10, 2001 to November 14, 2001, and had measured velocities ranging from 0.87-4.10 ft/s. For the 20 measurements, linear regression results in the following equation.

$$V_{Mean} = 0.8263V_{Index} + 0.0228 \tag{18}$$

Equation 18 provides a good fit to the data set. Equation 18 has a strong correlation with the data having a coefficient of determination of  $R^2 = 0.99$ .

With linear regression providing a good velocity rating, the same 20 velocity measurements are used to calibrate Equation 15. By minimizing the sum of the squared differences, the  $K$  value for the 20 measurements is found to be 4.65. Substitution of  $K$  into Equation 15 results in the following model.

$$V_{Mean} = 4.65 \frac{y(V_{Index})}{5.4127y + 9.9421} \tag{19}$$

Equation 19 provides comparable results and also provides a good fit to the velocity data. The coefficient of determination for Equation 19 is almost the same with  $R^2 = 0.99$ .

Figure 11 provides a visual of the comparison of the two velocity ratings with the measured velocities. As seen with Figure 11, the plots are almost on top of each other and the measured velocity. This can be expected based on the similar  $R^2$  values.

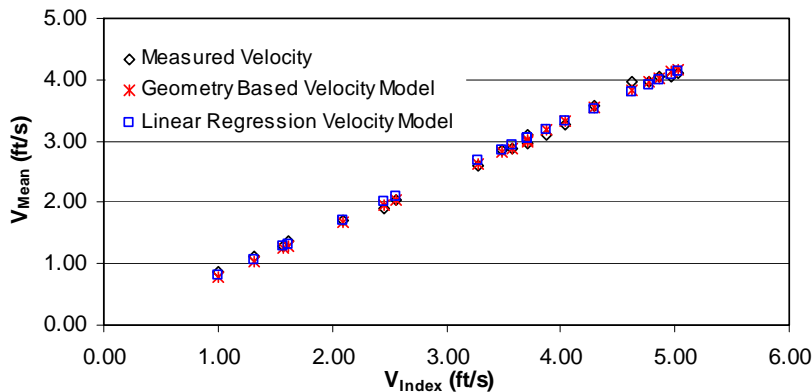


Figure 11. Comparison of the two velocity models to the measured velocity for the Red River at Grand Forks, ND.

Figure 12 further displays how well the two models fit the measured data. There does appear to be a trend for both models to under estimate velocities at the lower end and over estimate the mid rating velocities. With a standard error of 0.07 for both models, a conclusion can be made that both ratings have a good fit with the data used for calibration.

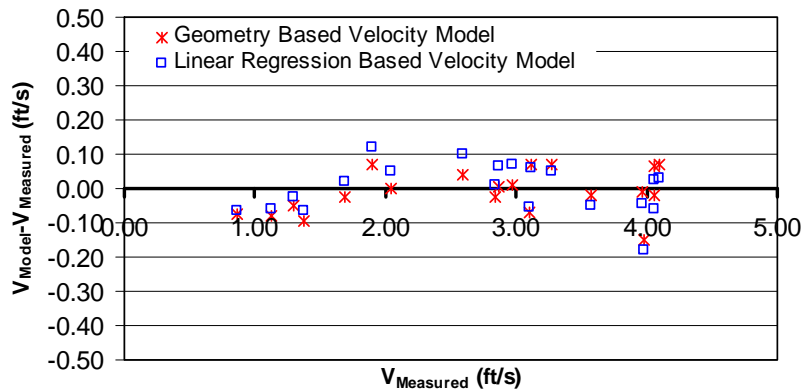


Figure 12 Plot of the difference between the computed velocity and the measured velocity against the measured velocity for the Red River at Grand Forks, ND.

**Application of the Two Velocity Ratings for Predicting Additional Measured Velocities**

With velocity rating developed for both methods and both methods showing comparable results, the two ratings are to be compared to see how well they can predict the mean channel velocities of the subsequent 45 measurements. The comparison of how well the two rating’s computed velocities match up with the measured velocities can be seen in Figure 13. As seen with Figure 13, both models tend to follow just below the trend laid out by the measured velocity. Both models maintain similar correlation with the data with both having an  $R^2$  value of 0.97.

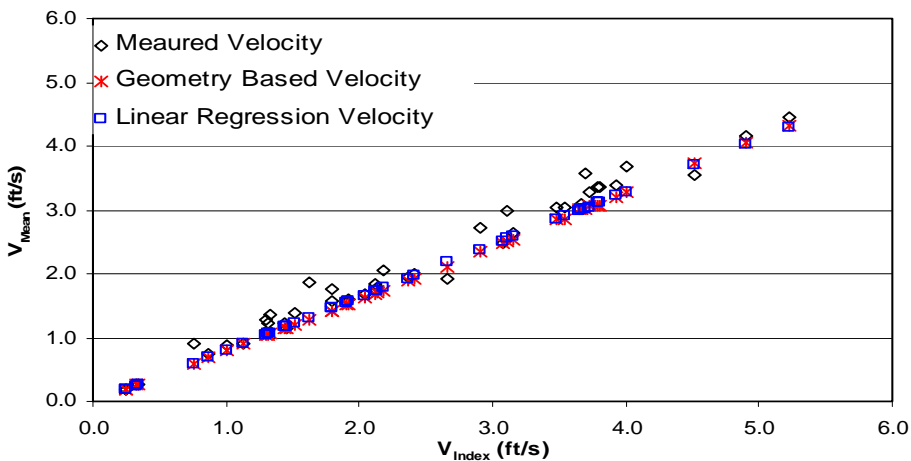


Figure 13. Comparison of the computed velocities from the two models to the measured velocities collected subsequent to the calibration data for the Red River at Grand Forks, ND.

As seen with Figure 13, the velocity rating derived through linear regression provides results comparable to those provided by the channel geometry based velocity rating. Both ratings tend to underestimate the measured velocity. The bias of underestimating the velocities can further be seen with Figure 11. The amount of deviation from the measured velocity can be seen with the shift in the standard error of the two models. The standard error for the two ratings increased

from 0.07 with data used for calibration to 0.23 and 0.22 for the channel based rating and linear regression rating respectively.

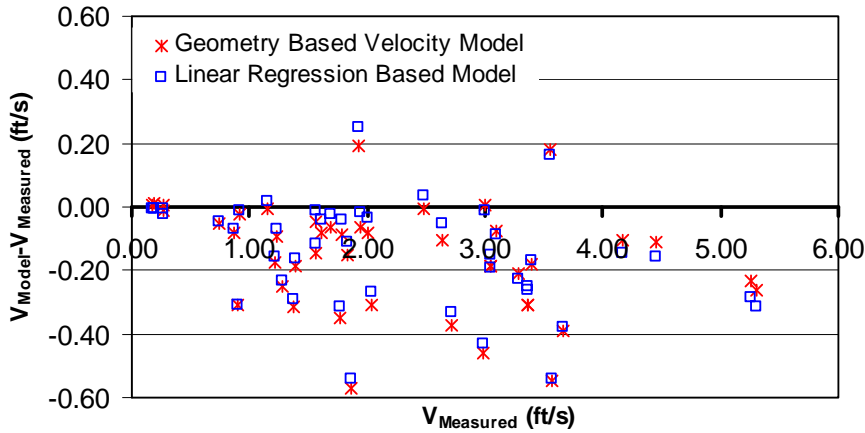


Figure 14. Plot of the difference between the computed velocity and the measured velocity against the measured velocity collected after the calibration data for the Red River at Grand Forks, ND

### Kankakee River at Davis, IN

The Kankakee River is part of the Illinois River basin with its head waters in northwestern Indiana (Morlock *et al.*, 2002). From there, the Kankakee flows in a generally westerly direction until it meets up with the Des Plains River. The merger of the two rivers forms the Illinois River as seen in Figure 15. To aid in estimating the discharge of the Kankakee River, an ADVM was installed in June of 1999 at the USGS gaging station, Kankakee River at Davis, IN. As previously mentioned, three sites were selected as a test site for the feasibility of ADVM's in discharge estimation. Kankakee River at Davis was one of the sites selected for the study. The data used for this study is a combination of the data reported in Morlock *et al.* (2002) and measurement data collected after the reported data.



Figure 15. Map of the Kankakee River adapted from U.S. Geological Survey Landsat imagery obtained from Google Earth<sup>TM</sup> in 2007.

### Channel Geometry of the Kankakee River at Davis, IN

The Kankakee River cross-section selected for the stage-area rating is rectangular by shape as seen with Figure 16. This cross-section was selected due to its uniform depth and geometry ((Morlock *et al.*, 2002). This rectangular geometry results in a linear stage-area rating. The area:depth ratio, or  $b$ , is needed for the calibration of the theoretical model of the index-mean velocity relationships within rectangular channels. Taking into account the effects of an uneven channel bed, the average  $b$  was found to be 46.21

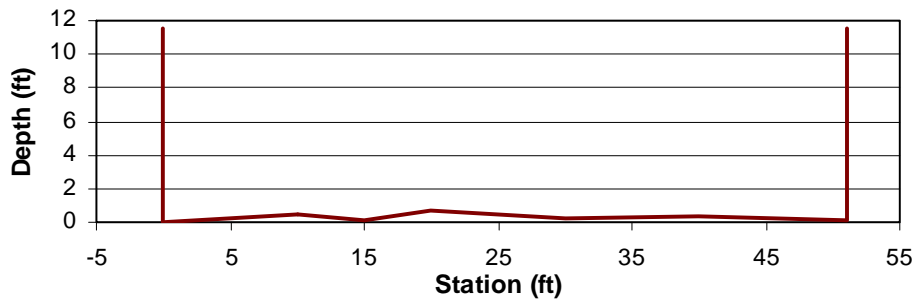


Figure 16. Profile of the Kankakee River's channel at Davis, IN.

### Channel Geometry-Based Velocity Rating for the Kankakee River at Davis, IN

Figure 16 shows that the channel cross-section for the Kankakee River at Davis, IN has a rectangular shape. Based on the channel's geometric shape, the theoretical model for rectangular index-mean velocity relationships is used to develop a velocity rating for the channel. Using the velocity data collected from the Kankakee River at Davis, IN, Figure 17 shows a graphical representation of the index-mean velocity relation found within the channel. As seen with Figure 17, the relationship between the index velocity and the corresponding mean velocity is nonlinear. This trend is consistent with observations discussed earlier for rectangular channels. Observation of the index-mean velocity relation displayed with Figure 17 shows that when the index velocity is equal to zero, the mean channel velocity will be greater than zero. Derived from this observation, the theoretical model for rectangular channels, Equation 10, is modified to include an intercept constant as shown with Equation 20.

$$V_{Mean} = K \frac{y(V_{Index})}{w} + c \quad (20)$$

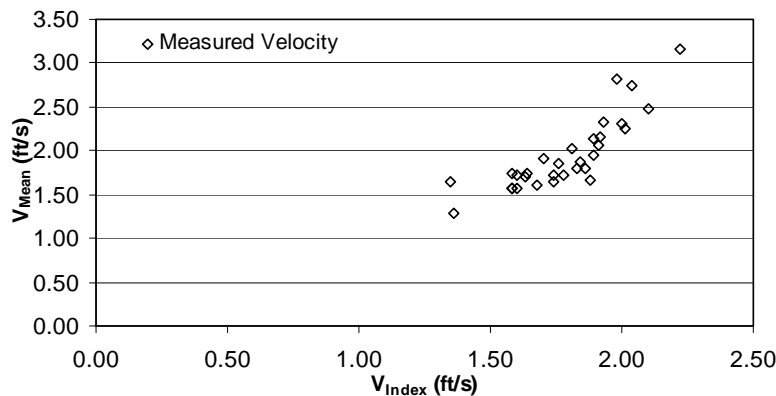


Figure 17. Index-mean velocity relation for the Kankakee River at Davis, IN.



Further observation of the velocity data shown in Figure 17 estimates the mean velocity to be around 1.0 ft/s when the index velocity is a zero. This value, 1.0 ft/s, is substituted for  $c$  in Equation 20 and 46.21 ft is substituted for  $w$ . These substitutions result in the Equation 21.

$$V_{Mean} = K \frac{y(V_{Index})}{46.21} + 1.0 \quad (21)$$

With  $c$  set to 1.0,  $K$  is derived by minimizing the sum of the squared difference between the measured velocity and the computed velocity. Iterations of this process are carried out by adjusting  $c$  to find the best  $K$  and  $c$  values for the model. These regression processes resulted in a  $K$  value of 5.15 and an intercept constant of 0.99. Substituting these values into Equation 20 results in Equation 22.

$$V_{Mean} = 5.15 \frac{y(V_{Index})}{46.21} + 0.99 \quad (22)$$

Equation 22 is the calibrated index-mean velocity rating for the velocity data displayed in Figure 17. Using Equation 22, the mean channel velocity is computed for each index velocity collected and corresponding depth within the channel. A comparison is then made between the velocities computed from Equation 22 and the mean velocities measured in the channel. Figure 18 displays how well the computed velocity matches the measured velocity.

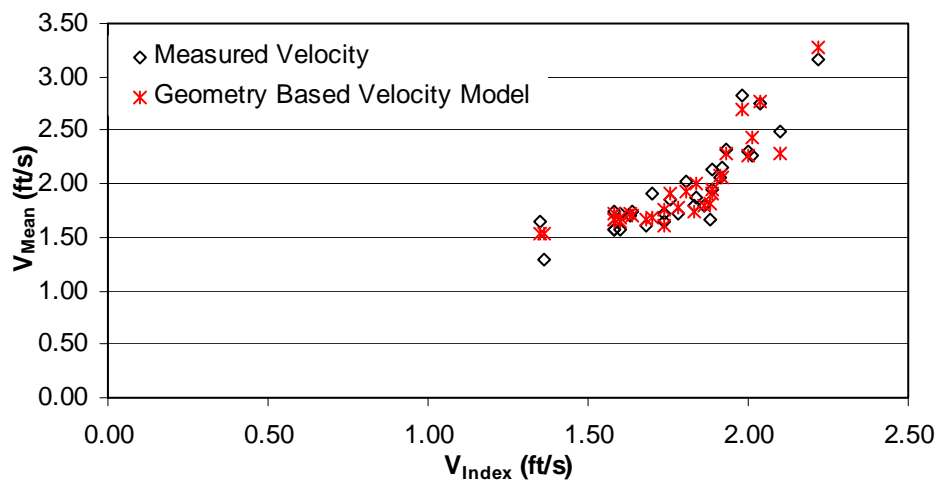


Figure 18. Comparison of modeled velocity to measured velocity for the Kankakee River at Davis, IN.

As seen with Figure 4.18, the index-mean velocity rating provides a fairly good fit to the measured velocity data. The coefficient of determination for the Equation 22 is found to be:  $R^2 = 0.93$ . This shows a good correlation between the model and the measured data, especially considering the amount of scatter with the measured velocity.

The goodness of fit for Equation 22 can be seen with Figure 19. Overall Equation 22 provides a favorable fit to the data with no clear bias of over or under estimating the measured velocity. For the velocities computed with Equation 4.9, the standard error is found to be 0.11.

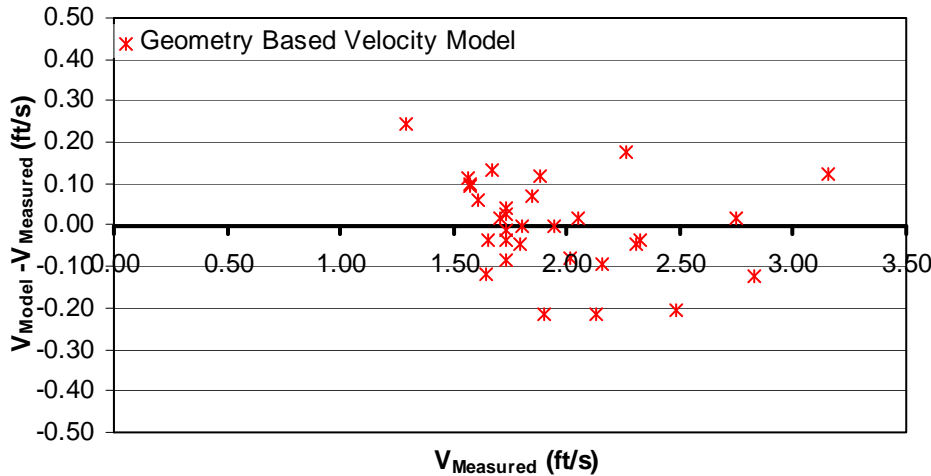


Figure 19. Comparison of the difference between the modeled velocity and measured velocity against the measured velocity for the Kankakee River at Davis, IN.

### **Comparison of the Channel Geometry-Based Velocity Rating and the Established Rating for the Kankakee River at Davis, IN**

As earlier mentioned, the study conducted by Morlock *et al.* (2002) showed that simple linear regression does not provide a desirable model of the index-mean velocity relation for rectangular channels. To model the index-mean velocity relation within the channel, Morlock *et al.* (2002) found stage to be a factor. To account for this, multiple linear regression was used with index velocity and stage as independent variables. This velocity rating developed through multiple linear regression is compared to the channel geometry-based index-mean velocity model. For this comparison, both velocity ratings are calibrated using the same data sets.

To develop the initial velocity rating for the Kankakee River at Davis, IN, Morlock *et al.* (2002) used 11 pairs of index and mean velocity measurements. A velocity model was fitted to the index-mean velocity relation using multiple regression. Using the model given by Hittle *et al.* (2001), with stage and the index velocity as independent variables, the regression equation derived by Morlock *et al.* (2002) is given by Equation 23.

$$V_{Mean} = V_{Index} (0.521 + 0.072H) + 0.102 \quad (23)$$

The same 11 measurements from June 30, 1999 to Feb. 27, 2001 were used to develop a channel geometry-based model for the index-mean velocity relationship. To find the best fit for Equation 4.7 and the 11 velocity measurements, iterations are carried out by adjusting  $c$ . For each adjustment of  $c$ , the corresponding  $K$  is derived by minimizing the sum of the squared differences. After conducting the iterations, Equation (24) is derived.

$$V_{Mean} = 4.68 \frac{y(V_{Index})}{46.21} + 1.13 \quad (24)$$

With the two ratings now derived, a comparison is made of the two modeling methods as seen with Figure 20. The multiple-linear method has a slightly stronger correlation with the velocity data though with an  $R^2$  value of 0.97. The channel geometry-based velocity model has a coefficient of determination somewhat lower at 0.96.

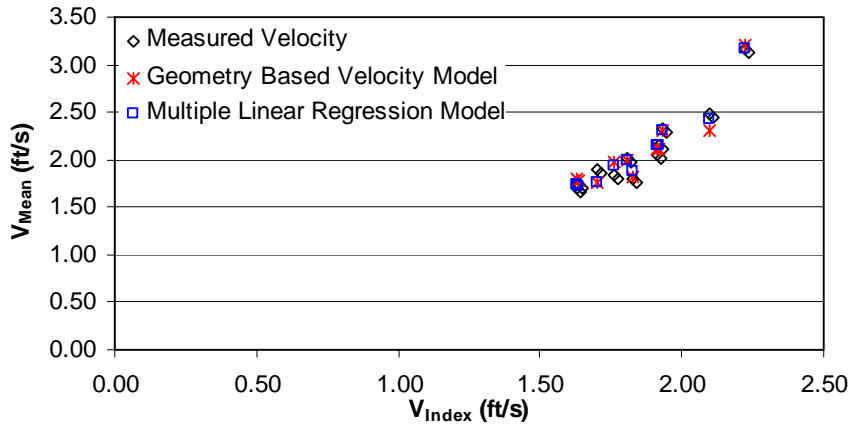


Figure 20. Comparison of the two velocity models to the measured velocity for the Kankakee River at Davis, IN.

Figure 21 provides another look at how well the computed velocities from the two models compare to the velocities measured within the channel. The overall fit of the two models with the measured velocity is favorable, showing no clear bias in the estimation of the measured velocity. The standard deviation of error for the geometry-based model and the multiple linear regression model are 0.10 and 0.08 respectively.

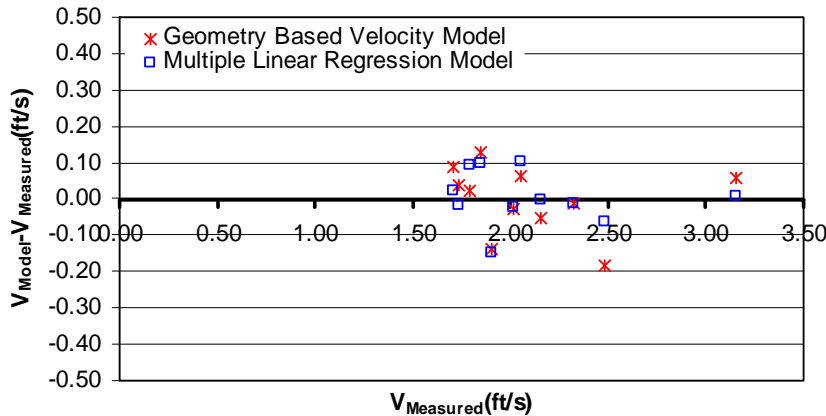


Figure 21. Plot of the difference between the computed velocity and the measured velocity against the measured velocity for the Kankakee River at Davis, IN.

### Comparison of the Two Velocity Ratings for Predicting Measured Velocities

Next the two rating, Equation 23 and 24, are compared using 19 velocity measurements collected after the data used for the calibration of the models. As seen with Figure 22, both ratings continue to compute velocities similar to one another. This also results in similar divergence from the measured velocity as both models tended to overestimate the mean velocity of the channel. Both models also have a similar correlation to the velocity data with both ratings having a coefficient of determination of  $R^2=0.86$ .

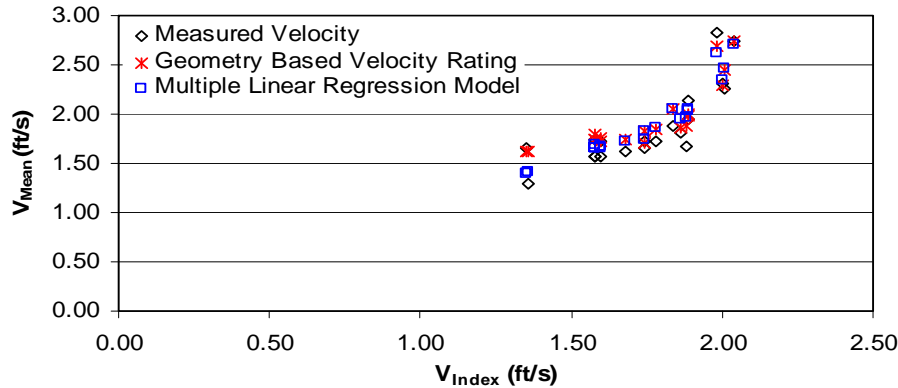


Figure 22. Comparison of the computed velocities from the two models to the measured velocities collected subsequent to the calibration data for the Kankakee River at Davis, IN.

The tendency for the two models overestimating the measured velocity is further displayed with Figure 23. For this site, neither of the two models is able to accurately define the index-mean velocity relation over time. This could possibly be attributed to transitions occurring with other parameters within the channel, of which, consequently affect the index-mean velocity relation. For the data set though, both model do not show a drastic increase in standard error. The standard error for this data set is 0.15 for both of the models.

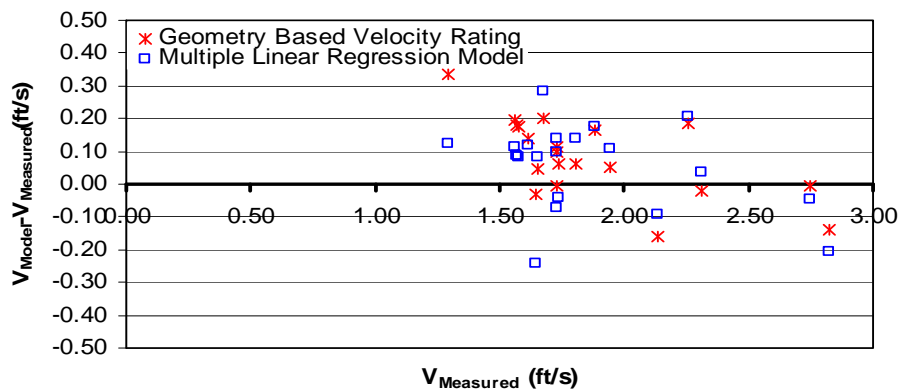


Figure 23. Plot of the difference between the computed velocity and the measured velocity against the measured velocity collected after the calibration data for the Kankakee River at Davis, IN.

## James River at the ND-SD Stateline

The James River is located within the Missouri River basin, originating from within Wells County, ND. From there, the river meanders at a generally southeasterly direction traveling through southeastern North Dakota and eastern South Dakota as seen in Figure 24. Along the river's 700 mi, there are numerous dams that have been constructed for water management purposes. One of these dams is the Sandhill Dam that is located in Brown County, SD. Variations within the stage of this reservoir result in variable backwater within the river along the North Dakota/South Dakota border. In addition, especially during low flows, the pooling effect of the reservoir also results in flows that are heavily affected by the wind. Therefore, to better monitor the discharge within this reach of the river, the stream-gage station, James River at the ND-SD state line, was selected to be equipped with an ADVIM.

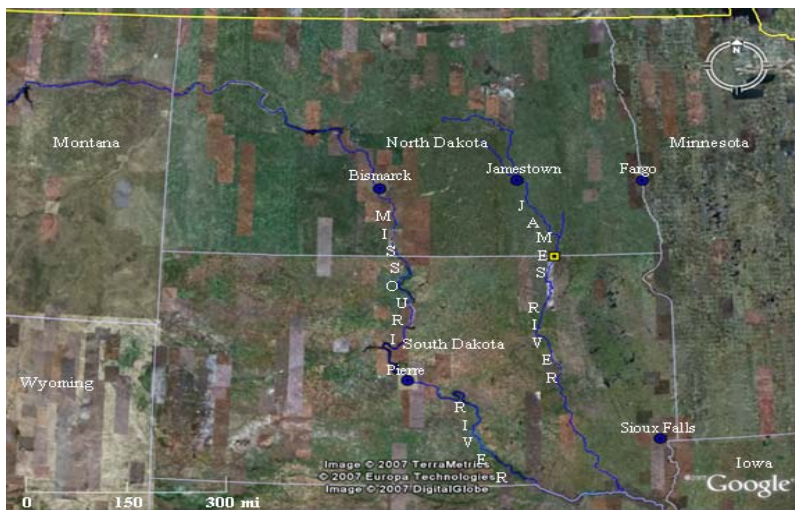


Figure 24. Map of the James River adapted from U.S. Geological Survey Landsat imagery obtained from Google<sup>TM</sup> Earth in 2007.

### Channel Geometry of the James River at the ND-SD State Line

The James River at the ND-SD state line has a generally wide channel bed with sloping banks. The ADVIM for this station, like the previous two sites, is located within a bridge constriction on the ND-SD state line. The abutments of the bridge shape the channel into more of a rectangular form. Even with the constriction, the channel is still fairly wide in comparison to the depths experienced as seen with Figure 25.

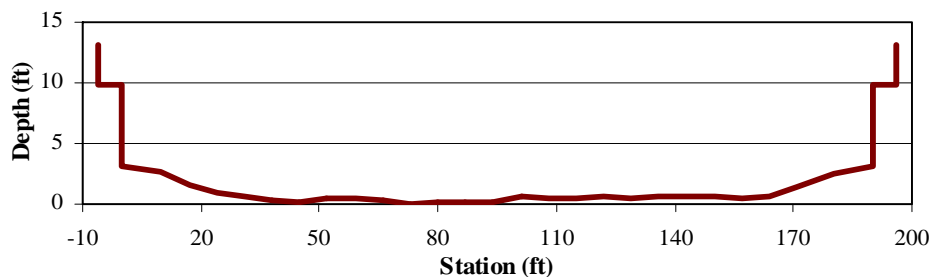


Figure 25. Profile of the James River's channel at the ND-SD state line.

For the James River at the ND-SD state line, as with the Kankakee River at Davis, IN, the uneven channel bed of the James River at the ND-SD state line results in an increasing area:depth ratio with an increase in depth. Therefore the average of the area:depth ratio will be used for the model. The average area:depth ratio,  $b$ , was found to be 155.14.

**Channel Geometry-Based Velocity Rating for the James River at ND-SD State Line**

Since the cross-section is a rectangular shape, Equation 10 is used as the theoretical model for the index-mean velocity rating. Using the velocity data collected for the James River at the ND-SD state line, Figure 26 shows a graphical representation of the index-mean velocity relation found within the channel. As seen with Figure 26, the relationship between the index velocity and the corresponding mean velocity has a somewhat linear trend. This trend is not consistent with observations discussed earlier for rectangular channels. This may be due to all the velocity data occurring within range of stage of only 5 ft. This range of stage in addition to the considerable width of the channel has not allowed the nonlinear trend to become visually evident. The depth-area relation is linear though and the channel is rectangular in shape.

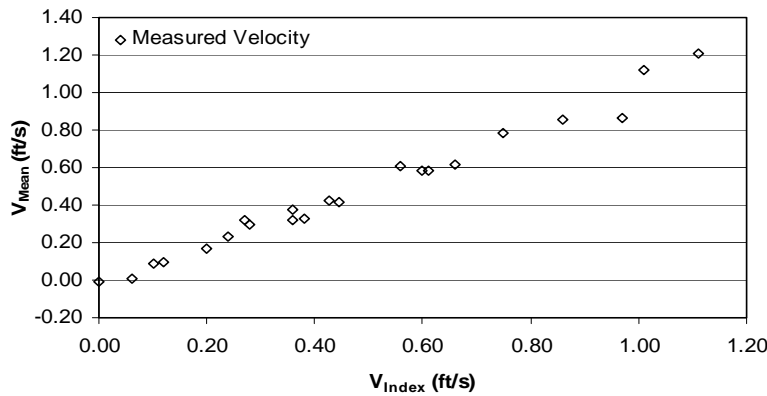


Figure 26. Index-mean velocity relation for the James River at ND-SD state line.

Unlike the previous rectangular channel, the Kankakee River at Davis, IN, the mean channel velocity goes to zero as the index velocity goes to zero. Based on this observation, an intercept is not required and therefore Equation 10 will be used as the theoretical model for the index-mean velocity relation. Calibration of the model is started by substituting the average  $w$  into Equation 10.  $K$  is once again derived by minimizing the sum of the squared difference between the measured velocity and the computed velocity. The  $K$  value derived through the regression process is 21.47. This value is substituted into Equation 10 deriving in Equation 25.

$$V_{Mean} = 21.47 \frac{y(V_{Index})}{155.14} \tag{25}$$

Equation 25 is the calibrated index-mean velocity rating for the James River at the ND-SD state line velocity data is displayed in Figure 26. A comparison is made between the computed

velocity from the model and the mean velocity measured in the channel. Figure 27 displays a visual view of how well the computed velocity matches the measured velocity.

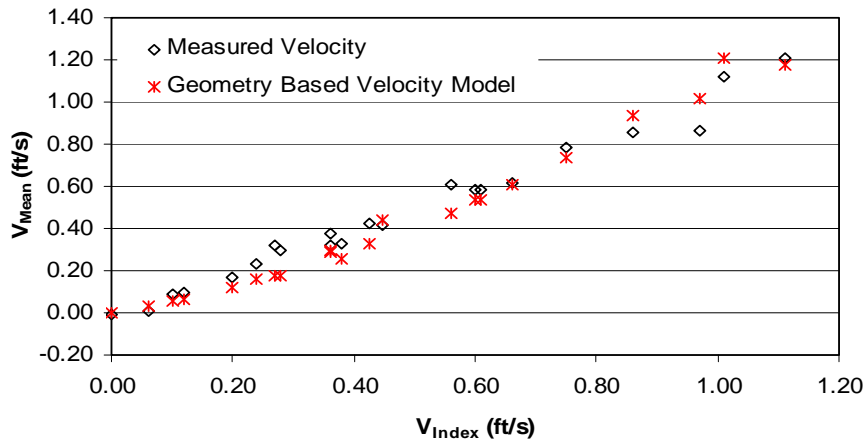


Figure 27. Comparison of modeled velocity to measured velocity for the James River at ND-SD state line.

As seen with Figure 27, the index-mean velocity rating under estimates the measured velocity data in the range of 0.2-0.6 ft/s. For velocities above 0.8 ft/s, the velocity model shows a tendency of overestimating the mean channel velocity. The coefficient of determination for the Equation 25 is found to be:  $R^2 = 0.94$  though. This shows a fairly good correlation between the model and the measured data. These are good results considering, as mentioned, how the flows within the channel are often heavily affected by the wind.

The biases displayed by the model are also seen with Figure 28. Figure 28 clearly shows the underestimation of the measured velocity within the mid range of velocities and overestimation of the measured velocities within the upper range of the rating. For this set of data, the model's standard error is relatively small though at 0.08.

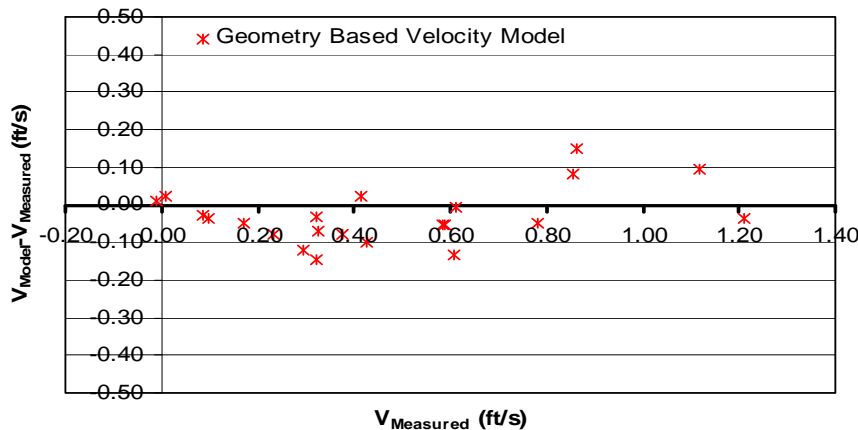


Figure 28. Plot of the difference between the computed velocity and the measured velocity against the measured velocity for the James River at the ND-SD state line.

**Comparison of the Channel Geometry-Based Velocity Rating and the Established Rating for the James River at ND-SD State Line**

As previous observation of Figure 26 has shown, the index-mean velocity relation displays somewhat of a linear trend. Morlock *et al.* (2002), as previously discussed, found that the index-mean velocity relation for many channels can be model by using simple linear regression. For the James River at ND-SD state line, linear regression has been the method used for modeling the relation. For this site, the channel geometry-based velocity model is compared to the velocity rating developed through linear regression.

To develop the first velocity rating for the James River at the ND-SD state line, 7 velocity measurements made during the summer of 2004 were used. These measurements had measured velocities ranging from 0.23-0.78 ft/s. Figure 29 shows the measured mean velocities vs. the measured index velocities for the given sample set.

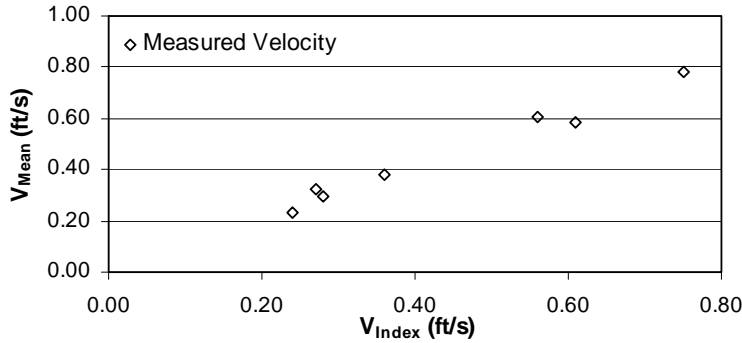


Figure 29. Index-mean velocity relation of the first 7 measured velocities for the James River at the ND-SD state line.

For the first 7 measurements used to develop the initial velocity rating, linear regression results in the following equation.

$$V_{Mean} = 1.0033V_{Index} + 0.0181 \tag{26}$$

Equation 26 provides a good fit to the data set and has a strong correlation with the data set. The coefficient of determination for Equation 4.14 is  $R^2 = 0.98$ .

Observation of the velocity data shows that the mean channel velocity does not go to zero when the index velocity goes to zero. Therefore, the modified version of Equation 10, Equation 20, is calibrated for the data set. Further observation of the velocity data estimates the intercept to be at about 0.10 ft/s. Using 0.10 ft/s as a starting point for  $c$ ,  $K$  is derived by minimizing the sum of the squared differences. The intercept  $c$  is then adjusted and iterations were carried out to obtain the  $K$  and  $c$  constants that best fit the model to the data. Using the iteration and regression processes, the  $K$  value for the 7 measurements is found to be 19.74 and the  $c$  value is 0.12 ft/s. Substitution of these values into Equation 20 results in the following model, Equation 27.

$$V_{Mean} = 19.74 \frac{y(V_{Index})}{155.14} + 0.12 \tag{27}$$



The channel geometry-based model, Equation 27, provides comparable results and also provides a good fit to the velocity data in comparison to the linear regression model. The coefficient of determination for the model is almost the same with  $R^2 = 0.97$ .

Figure 30 provides a visual of the comparison of the two velocity ratings with the measured velocities. As seen with Figure 30, the computed velocities are almost on top of each other and the measured velocity. This shows how well the goodness of fit is for the two models.

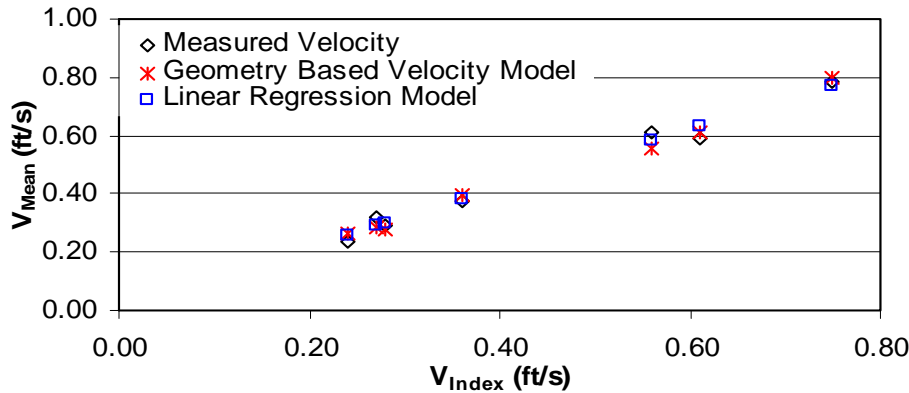


Figure 30. Comparison of the two velocity models to the measured velocity for the James River at the ND-SD state line.

The goodness of fit is also displayed with Figure 31. As seen with Figure 31, as with Figure 30, the two ratings can model the measured velocity used for the calibration quite well. This can be expected with the low standard deviation of error for the two models. The channel geometry-based model has a standard error of 0.04 while the linear regression model's standard error is slightly lower at 0.03.

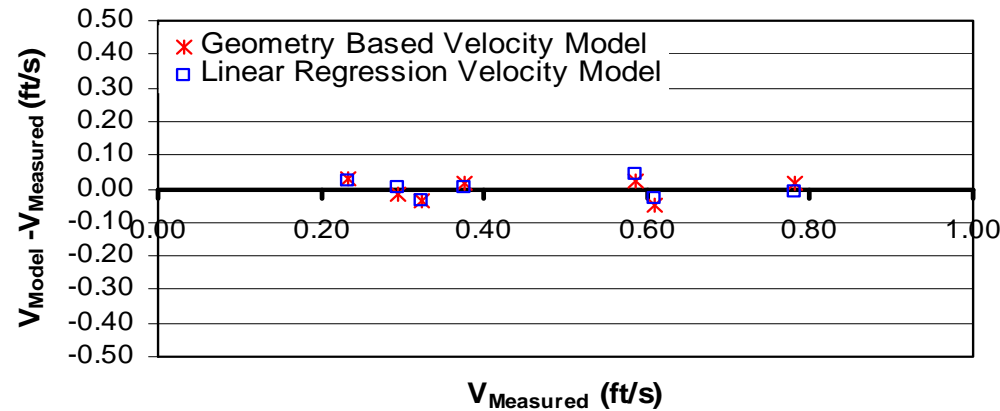


Figure 31. Plot of the difference between the computed velocity and the measured velocity against the measured velocity for the James River at the ND-SD state line.

### Comparison of the Two Velocity Ratings for Predicting Measured Velocities

Next the two rating, Equation 26 and 27, are compared using the 15 subsequent measurements. As seen with Figure 32, the linear regression velocity model has a tighter fit and produces a more accurate estimate of the measured velocity. This accuracy can be seen with the correlation coefficients. The linear regression model maintains similar coefficient of determination as before with  $R^2 = 0.97$ , while the channel geometry-based model's coefficient of determination drops off slightly to  $R^2 = 0.93$ .

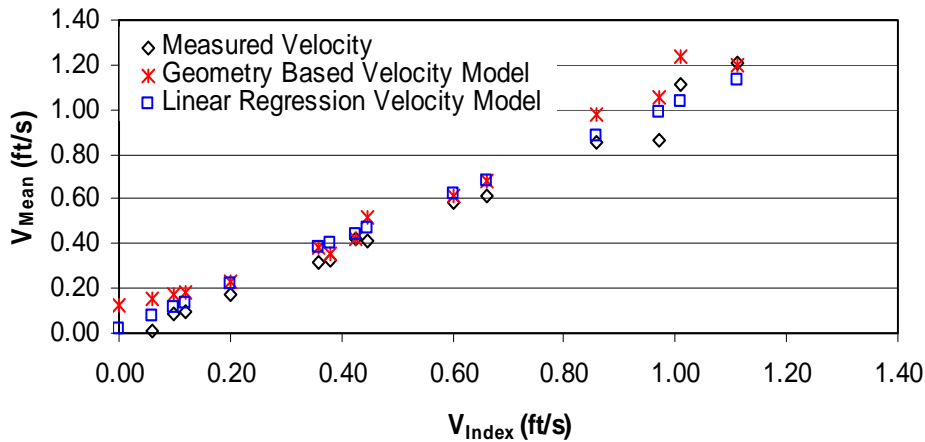


Figure 32. Plot of the difference between the computed velocity and the measured velocity against the measured velocity collected after the calibration data for the James River at the ND-SD state line.

The divergence of the two models from the measured velocity can be seen with Figure 4.33. As seen with Figure 4.33, both models are biased toward over estimating the measured velocity. The standard errors for the two models remain fairly low though. The channel based model has a standard error of 0.10 for this data set while the linear regression model has a standard error of 0.07.

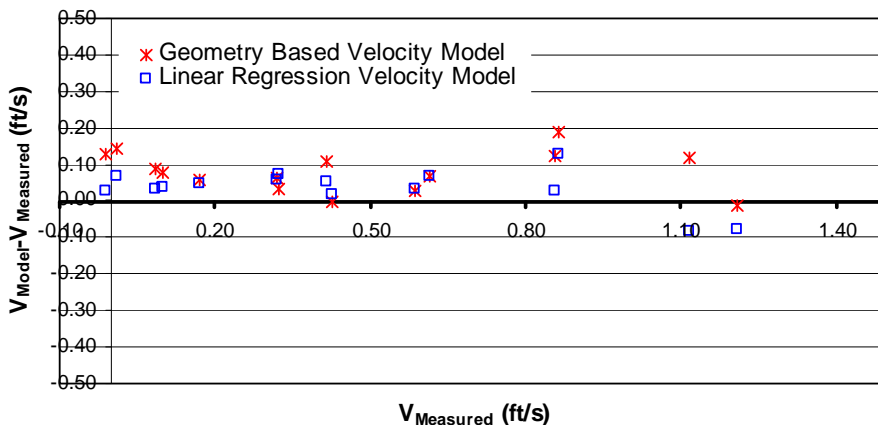


Figure 33. Plot of the difference between the computed velocity and the measured velocity against the measured velocity collected after the calibration data for the James River at the ND-SD state line.

## Kootenai River at Tribal Hatchery nr Bonners Ferry, ID

The Kootenai River originates in the Rocky Mountains in Southeastern British Columbia. From Within its 485 mi passage, the Kootenai experiences numerous channel bed transitions from steep bedrock in Montana to gentler sloped, sandy gravel from Idaho to Canada (Paragamian *et al.*, 2005). To aid in the estimation of discharge for the river, an ADVN was installed within the Kootenai River at the Tribal Hatchery near Bonners Ferry, ID.

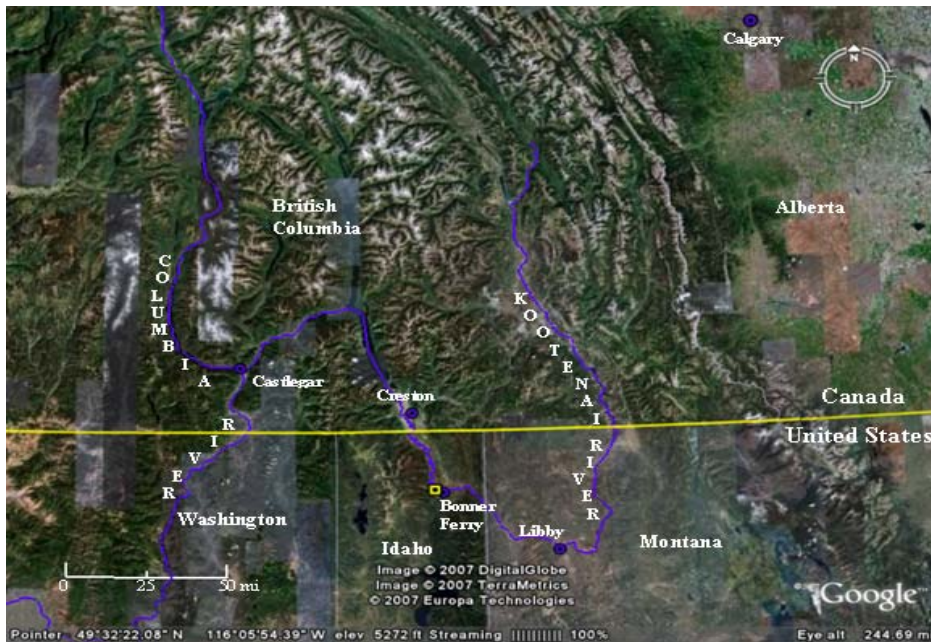


Figure 34. Map of the Kootenai River adapted from U.S. Geological Survey Landsat imagery obtained from Google<sup>TM</sup> Earth in 2007.

### Channel Geometry of the Kootenai River at the Tribal Hatchery Near Bonners Ferry, ID

Within this reach of the Kootenai River, the channel bed is considerably wide with sloping banks resulting in a generally trapezoidal cross-section as seen with Figure 35.

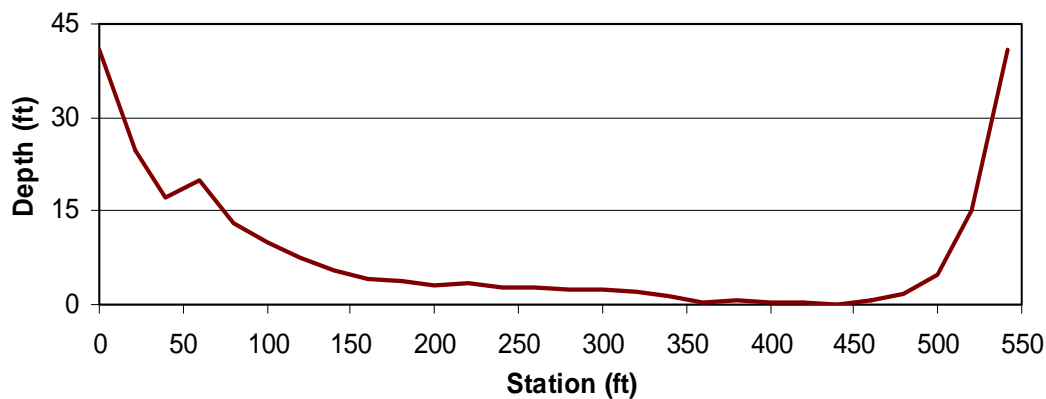


Figure 35. Profile of the Kootenai River at the Tribal Hatchery near Bonners Ferry, ID.

Figure 35 displays the trapezoidal shape of the channel cross-section for the Kootenai River. As seen with Figure 36 though, this cross-section provides a depth-area rating that displays a linear trend. This is due to the extreme width of the channel bed. For trapezoidal channels, the curvature of the depth-area relation decreases as the width of the channel bed increases. This is due to the area of flow above the channel's banks constitutes a small percentage of the overall area of the cross-section with a considerably wide bed. Consequently, this results in a linear depth-area relation.

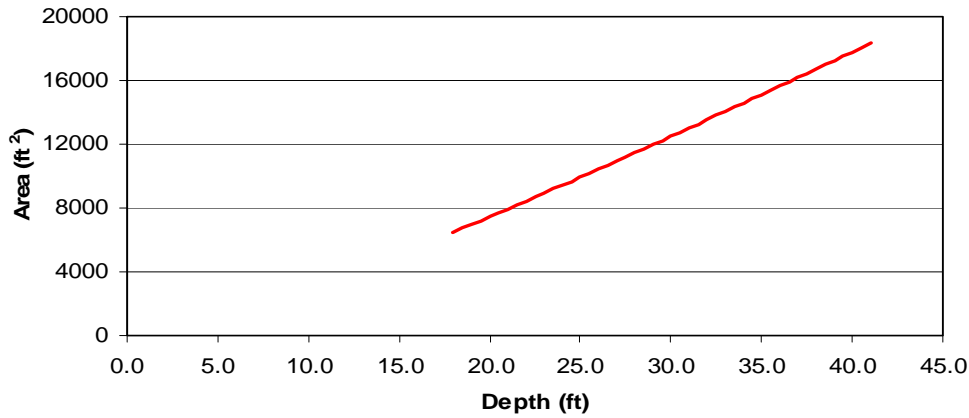


Figure 36. Depth-area rating for the Kootenai River at the Tribal Hatchery near Bonners Ferry, ID.

Since the channel has a trapezoidal shape, the depths and areas are used to fit the cross-section's data to the model given by Equation 13. Linear regression between the depth of flow and the corresponding area:depth ratio fits the data to Equation 13 model and results in Equation 28.

$$\frac{A}{y} = 3.6711y + 302.86 \quad (28)$$

Equation 28 generalizes the channel of the Kootenai River as shown in Figure 35 to have a channel bed width of around 303 ft. As seen with Figure 35 though,  $\theta_1$  is not equal to  $\theta_2$ . A constant and equal  $\theta$  is assumed for both banks though. With an  $m$  value of 3.6711, the average bank slope for the channel is  $15.2^\circ$ . Equation 28 does have a strong correlation with the range of data though, having an  $R^2$  value of 0.98. Using the average bank slope of  $15.2^\circ$  and the channel bed of 303 ft given by the Equation 4.16, a visual model of the channel is created. The model of the channel is compared to the channel cross-section given in Figure 35. The comparison of the original channel and the channel model can be seen with Figure 37. Both original cross-section and the model of the cross-section start at a station of 0.0 ft. For the given cross-section and stationing, the cross-section model estimates the channel to be about 60 ft wider than that given with the actual cross-section. With consideration given to the full width of the channel, the model provides a fairly good fit to the cross-section.

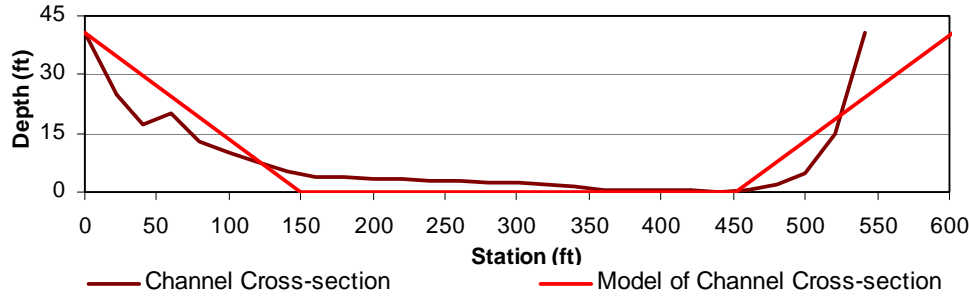


Figure 37. Comparison of the cross-sectional model to the layout of the cross-section.

### Calibration of the Channel Geometry-Based Velocity Rating

Using the velocity data collected for the Kootenai River at Tribal Hatchery near Bonners Ferry, ID, Figure 38 displays a graphical representation of the index-mean velocity relation found within the channel. As seen with Figure 38, the relationship between the index velocity and the corresponding mean velocity has a somewhat linear trend but starts to show a nonlinear relation with increasing velocities. This can again be attributed to the wide channel bottom. The width of the channel bed does not allow the theoretical model, Equation 11, to be simplified to a linear equation as with Equation 12. Therefore, a nonlinear relation can be expected.

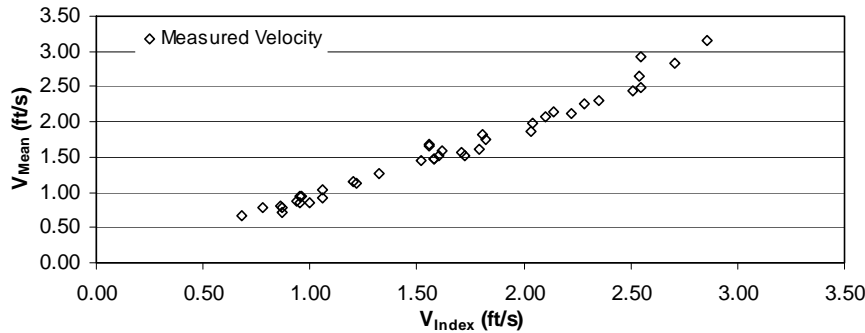


Figure 38. Index-mean velocity relation for the Kootenai River at Tribal Hatchery near Bonners Ferry, ID.

Equation 11 is used as the base theoretical model for the channel. Observation of the index-mean velocity relation displayed with Figure 38 shows that when the index velocity is equal to zero, the mean channel velocity is once again greater than the zero. Based on this observation, the theoretical model for trapezoidal channels is modified by adding an intercept as with the modification of the rectangular model, Equation 20. This modification results in Equation 29.

$$V_{Mean} = K \frac{(V_{Index})y}{(my + b)} + c \quad (29)$$

Further observation of the velocity data shown in Figure 38 estimates the mean velocity to be around 0.3 ft/s when the index velocity is a zero. This value, 0.3 ft/s, is substituted for  $c$  in Equation 29 along with Equation 28. Using an initial value of 0.3, the intercept value,  $c$ , is adjusted and iterations are carried out to find the  $K$  and  $c$  values through the method of least

squares. These regression processes result in a  $K$  value of 11.17 and an intercept constant of 0.35. Substituting these values into Equation 29 gives way to Equation 30.

$$V_{Mean} = 11.17 \frac{(V_{Index})^y}{(3.6711y + 302.86)} + 0.35 \quad (30)$$

As seen with Figure 39, the index-mean velocity rating provides a fairly good fit to the measured velocity data. The coefficient of determination for the Equation 30 is found to be:  $R^2=0.97$ . This shows a strong correlation between the model and the measured data, especially considering the amount of scatter with the measured velocity and the size of the channel.

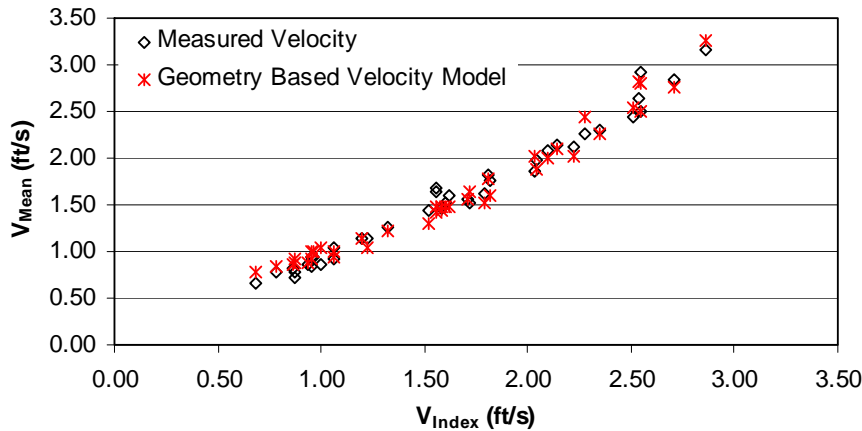


Figure 39. Comparison of modeled velocity to measured velocity for the Kootenai River at Tribal Hatchery near Bonners Ferry, ID.

The goodness of fit between Equation 30 and the measured velocity data is displayed with Figure 40. As seen by the scatter of the difference between the computed and measured velocities, the model does not display a trend of biasing towards over or under-estimating the mean channel velocity. Overall the model provides a good fit with the data having a standard deviation of error of 0.11.

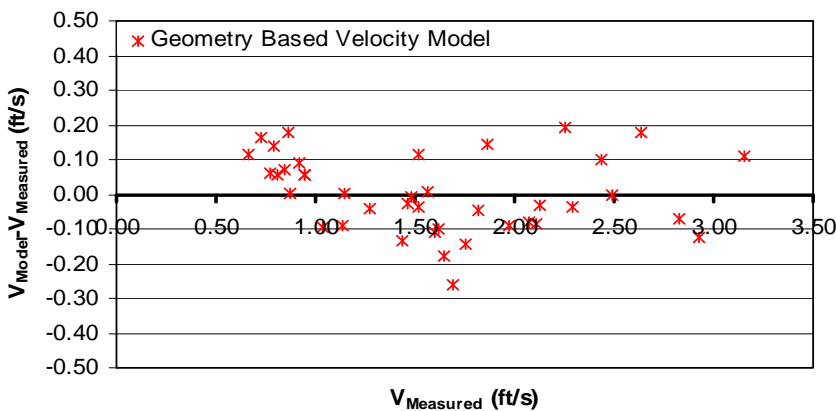


Figure 40. Plot of the difference between the computed velocity and the measured velocity against the measured velocity for the Kootenai River at Tribal Hatchery near Bonners Ferry, ID.

**Comparison of the Channel Geometry-Based Velocity Rating and the Established Rating for the Kootenai River at Tribal Hatchery Near Bonners Ferry, ID**

As with two of the three sites studied thus far, the index-mean velocity relations within the Kootenai River are modeled using linear regression. For this site, the channel geometry-based velocity model is compared to the velocity rating developed through linear regression. With this comparison, both velocity ratings are again calibrated using the same data sets.

To develop the first velocity rating for the Kootenai River at Tribal Hatchery near Bonners Ferry, ID, 10 velocity measurements made during the time period of October, 2002 to January 12, 2004 were used. These measurements had measured velocities ranging from 0.73-2.44 ft/s. Figure 41 shows the measured mean velocities vs. the measured index velocities for the given sample set.

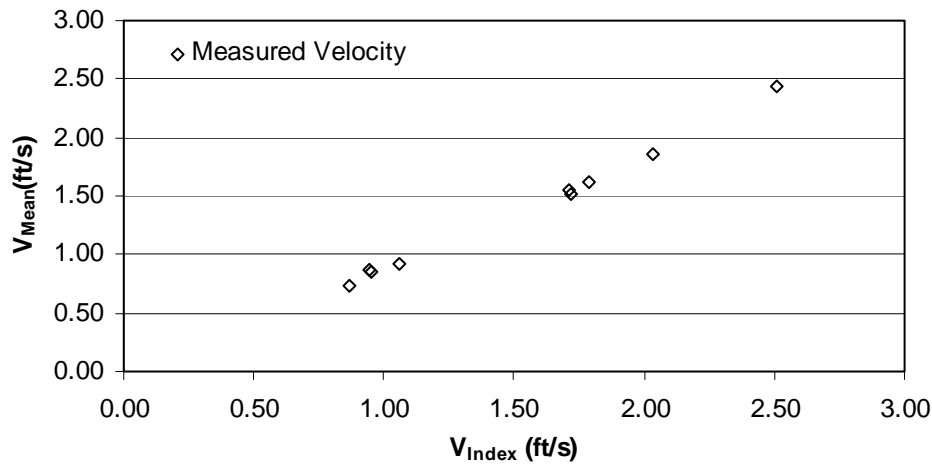


Figure.41. Index-mean velocity relation of the first 10 measured velocities for the Kootenai River at Tribal Hatchery near Bonners Ferry, ID.

Using the first 10 velocity measurements, the following equation is derived through linear regression.

$$V_{Mean} = 0.9906V_{Index} - 0.1225 \tag{31}$$

Equation 31 provides a very good fit to the data set having a strong correlation with the measured velocities. The coefficient of determination for Equation 4.20 is  $R^2=0.99$ .

For comparison purposes, the channel geometry-based velocity model is calibrated using the same 10 velocity measurements. Observation of the data shown in Figure 41 shows that the mean velocity is not equal to zero when the index velocity is equal to zero. Therefore, Equation 29 is used. The  $V_{Mean}$  intercept is estimated to be around 0.3 ft/s. Using 0.3 ft/s as an initial estimate for the intercept,  $c$  is adjusted to derive the  $K$  and  $c$  values that produce the minimal sum of the squared differences for the 10 measurements. The iterations result in a  $K$  value of 11.01 and an intercept of 0.30. Substitution of  $K$ ,  $c$  and Equation 28 into Equation 29 results in the following model, Equation 32.

$$V_{Mean} = 11.01 \frac{(V_{Index})y}{(3.6711y + 302.86)} + 0.30 \tag{32}$$

The channel geometry-based model, Equation 32, provides a good fit to the velocity data but does not have as strong of a correlation with the data as the linear regression model has. The coefficient of determination for the channel geometry-based model is  $R^2=0.98$ .

Figure 42 provides a graphical comparison of the two velocity ratings with the measured velocities. As seen with Figure 42, the computed velocities from the linear regression model match the measured velocities quite well. The channel based velocity model provides a fairly good fit to the measured velocity but has a little more drift from the measured velocity than the model derived through linear regression.

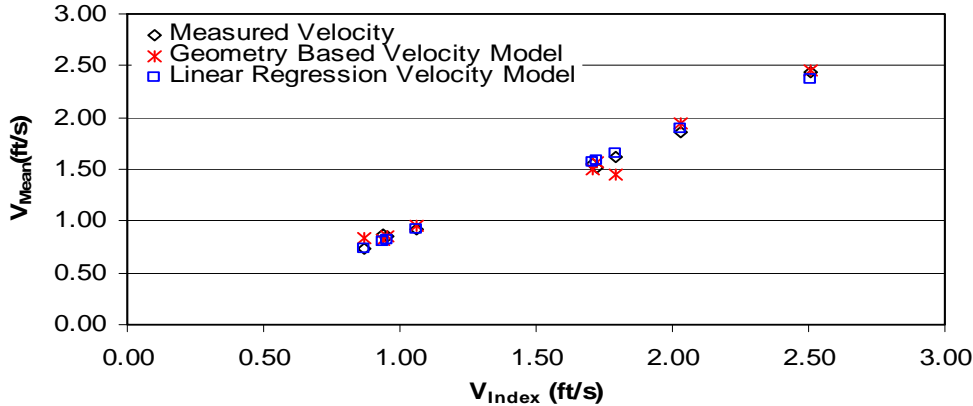


Figure.42. Comparison of the two velocity models to the measured velocity for the Kootenai River at Tribal Hatchery near Bonners Ferry, ID.

The goodness of fit for the two models can be seen in Figure 43. As seen with the graph, both models have a good fit with the data used for calibrating the model with no biases clearly evident. Figure 43 does show that the linear regression model has a tighter fit to the measured velocity than the channel based model. The standard error for the linear regression model is considerably low at 0.05 while the channel based model is slightly higher at 0.09.

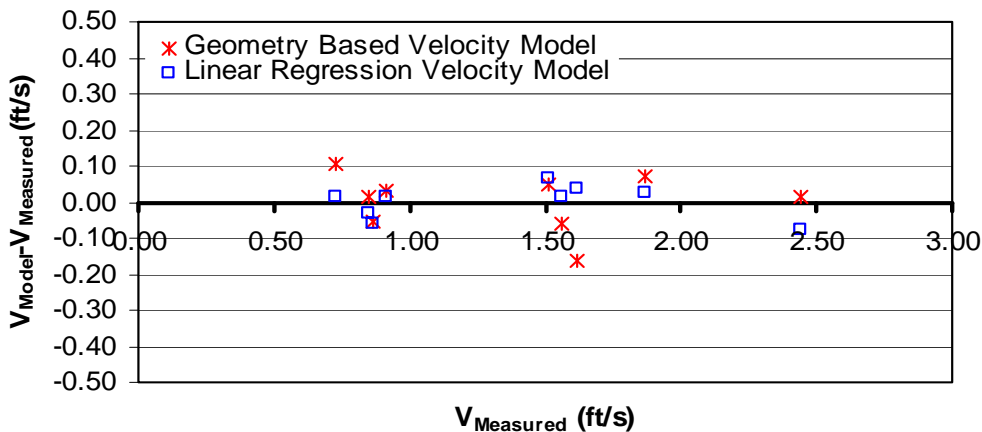


Figure 43. Plot of the difference between the computed velocity and the measured velocity against the measured velocity for the Kootenai River at Tribal Hatchery near Bonners Ferry, ID.



### Comparison of the Two Velocity Ratings for Predicting Measured Velocities

Using the 30 subsequent measurements made after the data sets used for calibrating the ratings, Equation 31 and 32 are compared to see how well they are able to predict the mean channel velocity. As seen with Figure 44, the channel geometry-based model provides a better fit to the measured velocity. The linear regression model tends to drift from the measured velocity above 2 ft/s while the channel geometry-based velocity model stays tighter. This drift can be attributed to the max velocity within the calibration data being only 2.44 ft/s. The velocity measurements conducted after the calibration data were as high as 3.16 ft/s. The better fit of the channel geometry-based model can also be seen with a stronger correlation of  $R^2=0.96$  while the linear model has a correlation of determination of  $R^2=0.93$ .

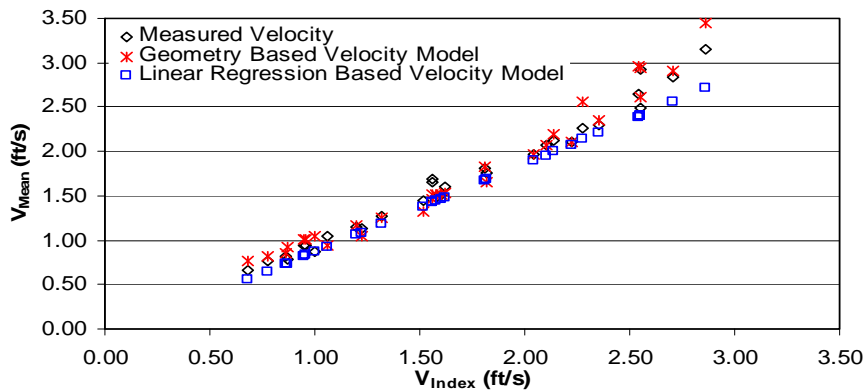


Figure 44. One to one comparison of the computed velocities to the measured velocities for the Kootenai River at Tribal Hatchery near Bonners Ferry, ID.

Figure 45 further displays the channel based model provides a better goodness of fit in comparison with the linear regression model. Both models have a fair amount of scatter but the linear regression model has a bias towards underestimating the mean channel velocity. The standard error for the linear regression model for the data set is 0.18. The channel geometry-based model conversely had a smaller increase from the calibration data set with a standard error of 0.13.

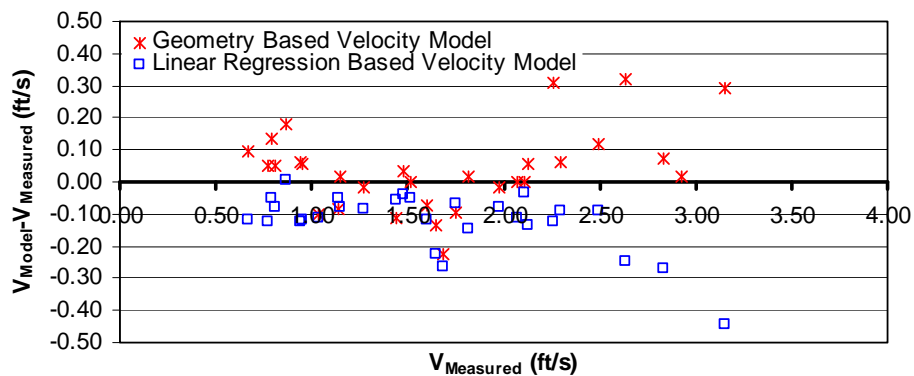


Figure 45. Plot of the difference between the computed velocity and the measured velocity against the measured velocity collected after the calibration data for the Kootenai River at Tribal Hatchery near Bonners Ferry, ID.

## Channel A near Penn, ND

Channel A is a man-made channel that connects two bodies of water in the northeast region of North Dakota. Located within Ramsey County, the 10 mi long channel connects Dry Lake to a northern bay of Devils Lake (Figure 46). Recent years have resulted in considerable backwater within the channel due to the overall continuous rise of Devils Lake, a semi-closed basin lake. With the exception of the spring rise from snow melt, the channel often experiences reverse flow, mainly driven by the wind.



Figure 46. Map of Channel A near Penn, ND and Big Coulee near Churches Ferry, ND adapted from U.S. Geological Survey Landsat imagery obtained from Google™ Earth in 2007.

During the summer of 2006, the flow of channel A was monitored as part of a Devils Lake hydraulic study. Since the channel is subject to bi-directional flow, an ADVN was used to aid in discharge computation.

### Channel Geometry of Channel A Near Penn, ND

The ADVN is located within a bridge constriction with vertical sides resulting in a cross-section that is rectangular in shape for the range of stage experienced. Figure 47 diagrams the channel profile. With the channel having a rectangular cross-section,  $w$  is computed for the range of stage that is expected. The uneven channel bed results in a  $w$  that is not constant for all stages. Therefore, the average is once again used. The average  $w$  is found to be 55.35.

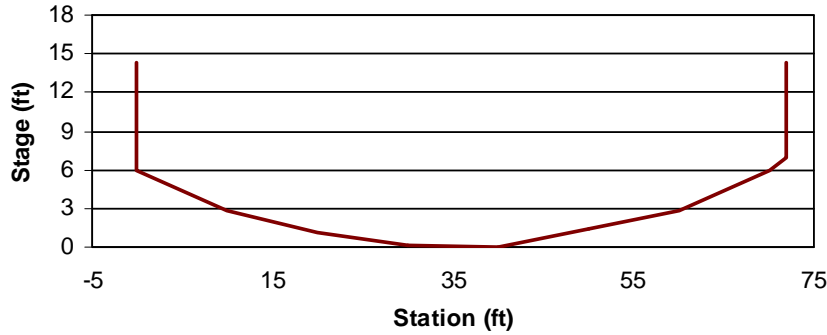


Figure 47. Profile of the channel cross-section for Channel A near Penn, ND

**Calibration of the Channel Geometry-Based Velocity Rating**

For this site, a total of 11 velocity measurements were conducted. Using the velocity data collected for Channel A near Penn, ND, Figure 48 displays a graphical representation of the index-mean velocity relation found within the channel. As seen with Figure 4.49, the relationship between the index velocity and the corresponding mean velocity once again has fairly linear relation. The range in depth experienced at the site is only 1.5ft. Based on this range of stage, the change is not significant and the nonlinear trend does not begin to take shape as expected. With the channel being rectangular though, Equation 10 is used as the model for the velocity relations.

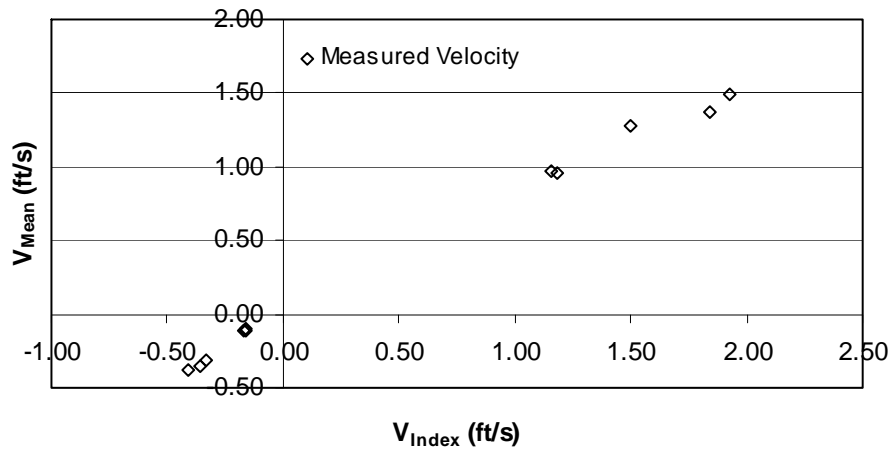


Figure 47. Index-mean velocity relation for Channel A near Penn, ND.

As seen with Figure 47, the mean velocity of the channel goes to zero as the channel’s index velocity goes to zero. Therefore, Equation 10 does not need to be modified and is used as the velocity model.

To start the calibration of the model, 55.35ft is substituted into Equation 10 for  $w$ .  $K$  is derived by minimizing the sum of squared differences between the measured and computed velocity data. For the velocity data at Channel A, the regression analysis results in a  $K$  value of 4.34. The substitution the  $K$  value of 4.34 into Equation 10 gives way to the following equation.

$$V_{Mean} = 4.34 \frac{y(V_{Index})}{55.35} \quad (33)$$

Equation 33 is the calibrated channel geometry-based velocity model for the velocity data collected for Channel A near Penn, ND. Figure 48 displays how well the model's computed velocity matches up with the measured velocity. Equation 33 has a good correlation with the measured data having a coefficient of determination of  $R^2=0.99$ . There does appear to be a trend though that the model under estimates the velocity that occurs during reverse flow.

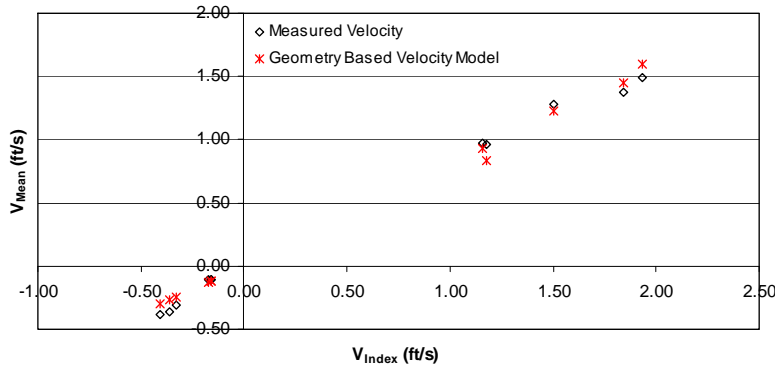


Figure 48. Comparison of the modeled velocity to measured velocity for Channel A near Penn, ND.

### **Comparison of the Channel Geometry-Based Velocity Rating and the Established Rating for Channel A Near Penn, ND**

For Channel A near Penn, the velocities of the channel were modeled using linear regression. For a comparison, a line is fitted to the 11 velocity data points shown in Figure 47 using linear regression. This process resulted in the following equation.

$$V_{Mean} = 0.8018(V_{Index}) + 0.0129 \quad (34)$$

Equation 34 is a rating curve that has a comparable fit to the measured velocity as that provided by the channel geometry-based model, Equation 33. This can be seen with Figure 4.49. As seen with the graph, the linear model also underestimates the velocity during reverse flow conditions. The linear model does have a good correlation with the measured velocity though also having a coefficient of determination of  $R^2=0.99$ , the same as the geometry-based model.

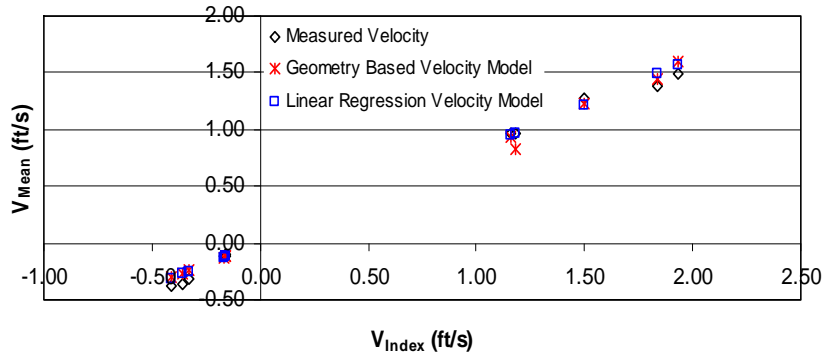


Figure 49. Comparison of the two velocity models to the measured velocity for Channel A near Penn, ND.

The goodness of fit for the two models can be seen with Figure 4.50. Both models seem to provide a good fit with the data set. The limited number of data points does not allow for the full analysis of any biases that the two models may have though. The standard error for the linear regression model and the geometry-based model are similar at 0.06 and 0.08 respectively.

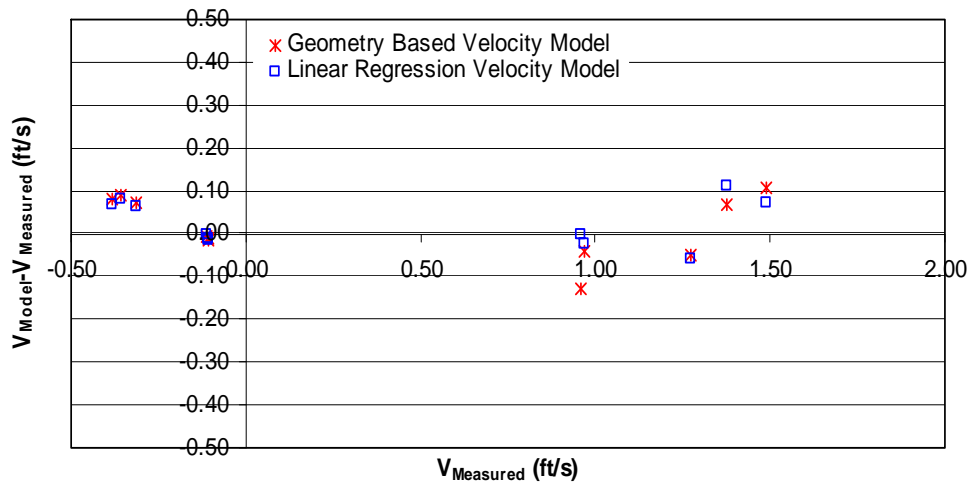


Figure 50. Plot of the difference between the computed velocity and the measured velocity against the measured velocity for Channel A near Penn, ND.

Due to the short duration of the study, there is a limited number of measured data. This has resulted in not having any measurements to compare the two ratings to see how accurate the two are for computing velocities not used in the calibration of the ratings. For the data provided for Channel A near Penn, ND, the two modeling methods provided favorable results with both of them computing a similar velocity and having especially similar correlation with the measured velocity.

### Big Coulee near Churches Ferry, ND

Referring back to Figure 46, Big Coulee is a channel that connects Lake Alice-Irvine to Devils Lake in the northeast region of North Dakota. Like Channel A, the rising water levels of Devils Lake over the past years have resulted in considerable backwater within the channel and

consequently periods of reverse flow occur. With the exception of the spring runoff, the direction of flow is as variable as the direction of the wind.

Along with Channel A, the discharge within Big Coulee was monitored during the summer of 2006, as part of the Devils Lake hydraulic study. Due to the channel being subject to backwater and reverse flow, an ADVN was used to aid in discharge computation.

**Channel Geometry of Big Coulee Near Churches Ferry, ND**

The ADVN is located within a bridge constriction with sloping banks forming a trapezoidal cross-section as seen with Figure 51.

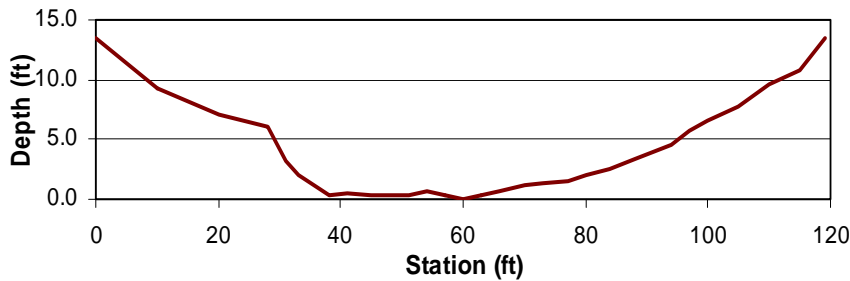


Figure 51. Profile of the channel cross-section for Big Coulee near Churches Ferry, ND.

The trapezoidal geometry of Big Coulee near Churches Ferry can also be seen with the nonlinear relation in the depth-area rating. As with the previous sites, the depth-area rating is developed by means of a cross-sectional survey. The relation for Big Coulee near Churches Ferry can be seen in Figure 52

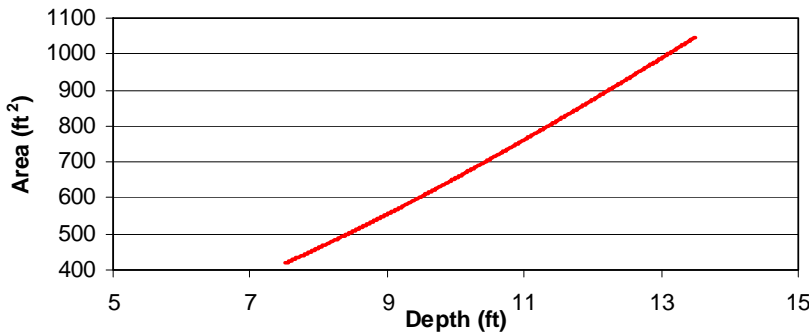


Figure 52. Depth-area rating for Big Coulee near Churches Ferry, ND.

The channel depths along with the corresponding areas are used to fit the data to the linear model given by 13. Linear regression between the depth of flow and the corresponding area:depth ratio fits the data to Equation 13 model and result in Equation 35.

$$\frac{A}{y} = 3.3857y + 32.01 \tag{35}$$

Equation 35 generalizes the channel of Big Coulee as shown in Figure 51 to have a channel bed width of 32ft. Assuming a constant  $\theta$  for both banks,  $m$  for Equation 35 equates an average bank slope of  $16.5^0$  for the channel. Equation 4.25 has a strong correlation with the data having an  $R^2$  value of 0.999.

Using the average bank slope of  $16.5^{\circ}$  and the channel bed of 32 ft given by the Equation 35, a model of the channel is created. The model of the channel is compared to the channel cross-section given in Figure 51. The comparison of the original channel and the channel model can be seen Figure 53. Both original cross-section and the model of the cross-section start at a station of 0 ft. For the given cross-section and stationing, the cross-section model estimates the channel to be about 4 ft wider than that shown with the actual cross-section. But as seen with Figure 53, the model of the cross-section provides a fairly accurate representation of the channel cross-section.

140

Figure 53. Comparison of the cross-sectional model to the layout of the cross-section for Big Coulee near Churches Ferry, ND.

**Calibration of the Channel Geometry-Based Velocity Rating**

The velocity data provided for Big Coulee show a linear relationship between the index velocity and the corresponding mean channel velocity. Figure 54 provides a graphical representation of the index-mean velocity relation found within the channel. The linear relation between the mean velocity measured in the channel and the index velocity measured by the ADVN is consistent with earlier observations for trapezoidal channels. As mentioned, Equation 11 is the theoretical model used to define the index-mean velocity relation within the channel.

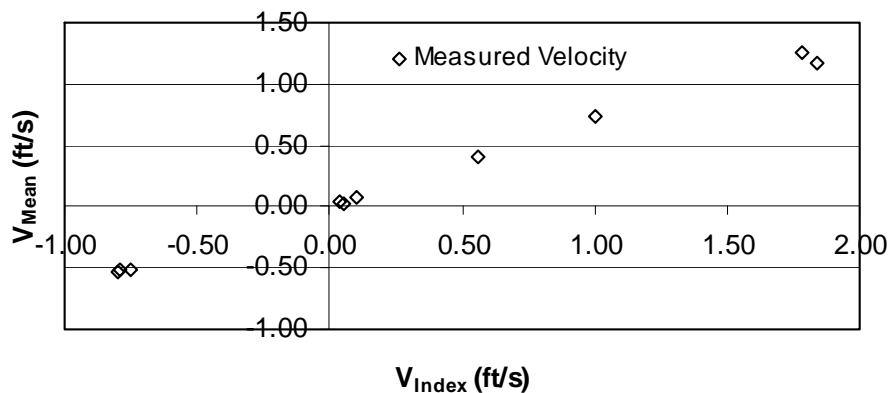


Figure 54. Index-mean velocity relation for the Big Coulee near Churches Ferry, ND.

Calibration of the geometry-based model for Big Coulee near Churches Ferry, ND begins with the substitution of Equation 35 into Equation 11. As with the previous sites the constant  $K$  for the data set is derived through the method of least squares. The  $K$  value derived through the regression is found to be 3.95. This value is substituted into Equation 11 resulting in Equation 36.

$$V_{Mean} = 3.95 \frac{y(V_{Index})}{3.3857y + 32.01} \quad (36)$$

Equation 36 is the calibrated index-mean velocity rating for the velocity data displayed in Figure 54. Using the model, the mean channel velocity is computed for each index velocity collected and corresponding depth within the channel. The computed velocity from Equation 36 is then compared to the mean velocity measured in the channel. This comparison can be seen in Figure 55. The index-mean velocity rating provides a good fit to the measured velocity data. The coefficient of determination for the Equation 36 is found to be  $R^2=0.996$ .

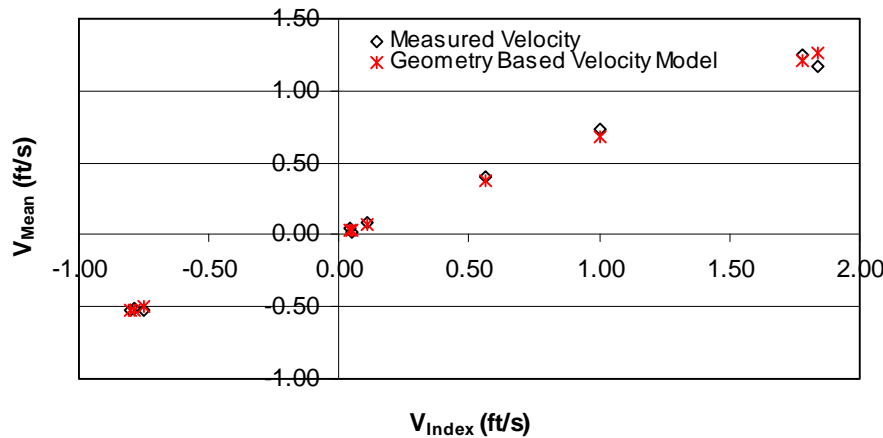


Figure 55. Comparison of modeled velocity to measured velocity for Big Coulee near Churches Ferry, ND.

Given the range of stage for Big Coulee has a difference of only 1.3 ft and a fairly wide channel bed, the bed width,  $b$ , does not become insignificant in velocity model. Therefore, Equation 4.27 can not be simplified to a linear equation. Equation 36 is used for comparison with the established method used for modeling the velocity relationships within Big Coulee near Churches Ferry, ND.

**Comparison of the Channel Geometry-Based Velocity Rating and the Established Rating for Big Coulee Near Churches Ferry, ND**

As with many of the channels covered earlier with this study, simple linear regression was used to model the index-mean velocity relations for Big Coulee. For comparison of the two models, the line that was derived for the same 10 sets of velocity data through linear regression is used. The linear model that was derived is given by Equation 37.

$$V_{Mean} = 0.672(V_{Index}) + .0099 \quad (37)$$



In comparison with the channel geometry-based model, Equation 36, Equation 37 provides almost the same results. This can be seen with Figure 56, where the computed velocities for the two models are practically plotted on top of each other. This can be explained in part by the correlation of the linear model with the measured data having the same coefficient of determination as Equation 37,  $R^2=0.996$ .

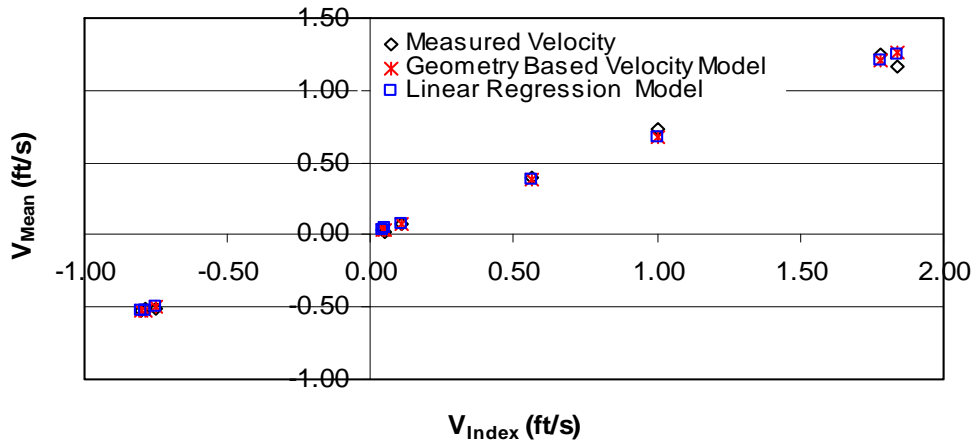


Figure 56. Comparison of the two velocity models to the measured velocity for Big Coulee near Churches Ferry, ND.

Figure 57 further displays the goodness of fit for the two models. For the amount of data, both models display similar results and have no clear bias. The standard error for the two models is the same at a low 0.04.

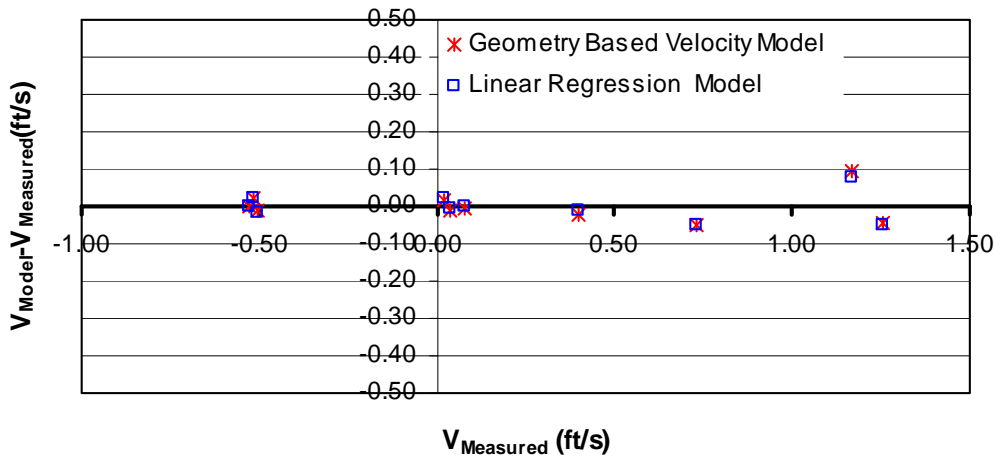


Figure 57. Plot of the difference between the computed velocity and the measured velocity against the measured velocity for Big Coulee near Churches Ferry, ND.

As with Channel A near Penn, ND, the short duration of the study resulted in limited number of measured data. This has resulted in not having any measurements to compare the two ratings to see how accurate the two are for computing velocities not used in the calibration of the ratings. For the data provided though, both methods of modeling the index-mean velocity relation provide similar results that are quite favorable.

## CONCLUSIONS

For the six sites used to test the channel geometry-based velocity models, the results proved to be quite favorable. Calibration of the velocity ratings based on the geometric characteristics of the channel's cross-section can allow for the development of a velocity rating more rapidly than the conventional methods presently used and offers a more theoretical reasoning to the rating. For each velocity rating, consideration needs to be given to the quality of the measurements used to derive the rating. As with the previous methods used, the accuracy of the geometry-based model increases as more measurements are conducted and the trends can be more clearly verified.

For the six sites used in the study, a velocity rating was derived based on the channel's geometry and all the velocity data provided. All the models had fairly strong correlation with the measured velocities. The lowest correlation with the measured data occurred with the Kankakee River at Davis, IN. At this site, the coefficient of determination was found to be  $R^2=0.93$ . All the five other sites had a stronger correlation with the given site's data, with three of the sites having an  $R^2$  value of 0.98 or higher

For comparison purposes, a channel geometry-based model was derived for each site using the same velocity measurements that were used to develop a velocity rating using conventional velocity rating development methods. The conventional method used for developing a velocity rating for five of the six sites was simple linear regression. The exception of the six is the Kankakee River at Davis, IN. At this site multiple linear regression was used to define the index-mean velocity relation. With the conventional velocity ratings given, a comparison was made between the conventional velocity rating and the rating developed based on the channel's geometry. Of the six sites, only the geometry-based model for the Red River at Grand Forks, ND had a stronger correlation with the measured velocity than the rating developed by conventional means. As for Channel A and Big Coulee, the two velocity ratings provided the same correlation with the measured velocity. Of the three remaining sites, all three have a weaker correlation with the measured velocity in comparison to the conventional velocity rating. The Kankakee River at Davis, IN has the weakest comparison of all the sites with an  $R^2$  value of 0.96. This is comparable though to the  $R^2$  value provide by the conventional rating at 0.97.

After the comparing the goodness of fit of the two ratings to the data used for calibration, the two rating were compared to see how well each model can predict the subsequent measured velocity for measurements conducted after the calibration of the two velocity ratings. Two of the six sites, Channel A near Penn, ND, and Big Coulee near Churches Ferry, ND, had a limited amount of data collected and could not be used for this comparison. Of the four sites used, only the Kootenai River at the Tribal Hatchery near Bonners Ferry, ID had a stronger correlation with the measured velocity than the conventional rating for the site. Two of the four had the same correlation with the data as the conventional rating. The channel geometry-based velocity rating for the James River at the ND-SD state line provided the least favorable results in comparison

with the conventional rating. While the conventional rating for this site maintained its correlation with the measured data after calibration, the geometry-based model's correlation with the data dropped slightly from an  $R^2$  value of 0.97 after calibration to a 0.93 correlation with the data collected after calibration. Overall though, as time passed, subtle transitions within the channel tended to result in similar drift between the computed velocity and the measured velocity for both ratings at each site. This is an expected occurrence within natural channels.

Of the geometry-based models, for the sites studied, the trapezoidal model provided more favorable results in comparison to the model for rectangular channels. After initial calibration, the geometry-based model for the trapezoidal channels had an average  $R^2$  of 0.99 for the calibration data, while the rectangular model had an average  $R^2$  value of 0.97. As for the four sites that had velocity data subsequent to the calibration of the velocity rating, the trapezoidal model had an average  $R^2$  value of 0.97 while the rectangular models had an average  $R^2$  value 0.90. Analysis of the sites do show a much more consistent trend in the index-mean velocity relationships the trapezoidal channels in comparison to the consistency of the velocity trends for the rectangular channel.

In general though, the geometry-based models explain the index-mean velocity relationships experienced in the field. For a channel with a trapezoidal geometry, in addition to estimating the channel's bank slopes and bed width, the model mathematically explains how the index velocity develops a linear relation with the mean channel velocity. For channels with rectangular geometry, the model defines how a non-linear relationship can develop between the index velocity and the corresponding mean channel velocity.

Overall though, the rating models using channel geometry, in comparison to the conventional methods used, can produce a fairly accurate rating for channels with trapezoidal or rectangular characteristics. One of the main strengths of the rating model is the incorporation of area and depth into the rating. The incorporation of these parameters allow for the development of a velocity rating with fewer measurements along with a reasonable degree of confidence in computing velocities that the rating range has not yet experienced.

There are numerous areas that can be further studied for this method of rating development. Further analysis is needed to better understand the properties of the  $K$  value of the ratings. Additional studies into how channel characteristics and the ADVN's location within the channel shapes this parameters can possibly lead to more accurate velocity ratings and potentially a theoretical rating that can be developed before a discharge measurement is even conducted.

Additional studies also need to be conducted to see how the models work in channels with complex channel beds and slopes. As mentioned, the channels used for this study have a fairly uniform channel bottom. Rivers and streams with numerous channels or flows into the established flood plains were not tested with this study.

## REFERENCE

- Google™ Earth. (2007). <http://earth.google.com/download-earth.html>. Version 4.2.0181.2634.
- Hittle, C., Patino, E., Zucker, M. (2001). “*Freshwater Flow From Estuarine Creeks Into Northeastern Florida Bay.*” U.S. Geological Survey Water Resources Investigations Report 01\_4264, 32P.
- Hirsch, R.M., Norris, J.M. (2001). “*National Streamflow Information Program Implementation Plan and Progress Report.*” U. S. Geological Survey Fact Sheet FS-048-01, 6 p.
- Huntley, H.E. (1955). “*Dimensional Analysis.*” Rinehart & Company Inc., New York, N.Y. 158 p.
- Mason Jr., R.R., and Weiger, B.A. (1995). “*Stream Gaging and Flood Forecasting.*” U. S. Geological Survey Fact Sheet FS-209-95, 3 p.
- Morlock, S. E., Nguyen, H. T., and Ross, J. H. (2002). “*Feasibility of Acoustic Doppler Velocity Meter for the Production of Discharge Records from U.S. Geological Survey Streamflow-Gaging Stations.*” U. S. Geological Survey Water-Resources Investigations Report 01-4157, 59 p.
- Paragamian, V.L, Hardy, R., Gunderman, B. (2005). “*Effects of Regulated Discharge on Burbot Migration.*” J. of Fish Biology, 66(5), 1199-1223.
- Rantz, S.E., and others. (1982a). “*Measurement and Computation of Streamflow.*” U.S. Geological Survey Water-Supply Paper 2175, 1v, 1-284.
- Rantz, S.E., and others. (1982b). “*Measurement and Computation of Streamflow.*” U.S. Geological Survey Water-Supply Paper 2175, 2v, 285-631.
- Ruhl, C.A., and Simpson, M. R. (2005). “*Computation of Discharge Using the Index-Velocity Method in Tidally Affected Areas.*” U.S. Geological Survey Scientific Investigations Report 2005-5004, 31 p.
- Sontek Corporation. (2004). “*Argonaut-SL Expanded Description.*” [www.sontek.com](http://www.sontek.com): San Diego, C.A. 5 p.
- Sloat, J.V., and Hull, M. (2004). “*Computing Discharge Using the Velocity-Index Method.*” SonTek-YSI Fact Sheet, 1-32.